Self-oligomerization regulates stability of Survival Motor Neuron (SMN) proteins by sequestering an SCF^{Slmb} degron

Kelsey M. Gray[a,b], Kevin A. Kaifer[d], David Baillat[e], Ying Wen[b], Thomas R. Bonacci[a,c], Allison D. Ebert[e], Amanda C. Raimer[a,b], Ashlyn M. Spring[b], Jacqueline J. Glascock[d], Sara ten Have[g], Michael J. Emanuele[a,c], Angus I. Lamond[g], Eric J. Wagner[e], Christian L. Lorson[d], and A. Gregory Matera[a,b]

Running title: SCF^{Slmb} mediates degradation of SMN

[a]Curriculum in Genetics and Molecular Biology and Lineberger Comprehensive Cancer Center, University of North Carolina, Chapel Hill, NC 27599, USA

[b]Integrative Program in Biological and Genome Sciences, Department of Biology and Department of Genetics, University of North Carolina, Chapel Hill, NC 27599, USA

[c]Department of Pharmacology, University of North Carolina, Chapel Hill, NC 27599, USA

[d]Molecular Pathogeneses and Therapeutics Program, Department of Veterinary Pathobiology, College of Veterinary Medicine, Bond Life Sciences Center, University of Missouri, Columbia, MO 65211, USA

[e]Department of Biochemistry and Molecular Biology, University of Texas Medical Branch, Galveston, TX 77550, USA

[f]Department of Cell Biology, Neurobiology and Anatomy, Medical College of Wisconsin, 8701 Watertown Plank Rd, Milwaukee, WI 53226, USA

[g]Centre for Gene Regulation and Expression, School of Life Sciences, University of Dundee, Dundee, DD15EH, UK

Address correspondence to: A. Gregory Matera
Integrative Program for Biological and Genome Sciences
Campus Box 7100
University of North Carolina
Chapel Hill, NC 27599
Voice: (919) 962-4567
FAX: (919) 962-4574

Abstract

Spinal muscular atrophy (SMA) is caused by homozygous mutations in human *SMN1*. Expression of a duplicate gene (*SMN2*) primarily results in skipping of exon 7 and production of an unstable protein isoform, SMNΔ7. Although *SMN2* exon skipping is the principal contributor to SMA severity, mechanisms governing stability of SMN isoforms are poorly understood. We used a *Drosophila* model system and label-free proteomics to identify the SCF^{Slmb} ubiquitin E3 ligase complex as a novel SMN binding partner. SCF^{Slmb} interacts with a phospho-degron embedded within the human and fruitfly SMN YG-box oligomerization domain. Substitution of a conserved serine (S270A) interferes with SCF^{Slmb} binding and stabilizes SMNΔ7. SMA-causing missense mutations that block multimerization of full-length SMN are also stabilized in the degron mutant background. Overexpression of $SMN\Delta7^{S270A}$, but not wild-type SMNΔ7, provides a protective effect in SMA model mice and human motor neuron cell culture systems. Our findings support a model wherein the degron is exposed when SMN is monomeric, and sequestered when SMN forms higher-order multimers.

Introduction

Spinal muscular atrophy (SMA) is a common neuromuscular disorder, recognized as the most prevalent genetic cause of early childhood mortality (Pearn 1980). Patients with the most severe form of the disease, which is also the most common, become symptomatic in the first six months of life and rarely live past two years (Wee et al. 2010; Prior 2010). Because the onset of symptoms and their severity can vary, SMA has historically been classified into three subtypes (Ogino and Wilson 2004). More recently, clinicians have recognized that SMA is better characterized as a continuous spectrum disorder, ranging from acute (prenatal onset) to nearly asymptomatic (Tiziano et al. 2013). Clinically, SMA patients experience degeneration of motor neurons in the anterior horn of the lower spinal cord (Crawford and Pardo 1996). This leads to progressive atrophy of proximal muscle groups, ultimately resulting in loss of motor function and symmetrical paralysis. The cause of death is often restrictive respiratory failure (Kolb and Kissell 2015).

SMA typically results from homozygous deletion of the *survival motor neuron 1* (*SMN1*) gene (Lefebvre et al. 1995). A small fraction of SMA patients have lost one copy of *SMN1* and the remaining copy contains a point mutation (Burghes and Beattie 2009). Humans have two *SMN* paralogs, named *SMN1* and *SMN2*, both of which contribute to total cellular levels of SMN protein. *SMN2* exon 7 contains a silent base change that alters splicing to primarily produce a truncated, unstable protein product called SMNΔ7 (Lorson et al. 1999; Monani et al. 1999; Lorson and Androphy 2000). The last 16 amino acids of SMN are replaced in SMNΔ7 by four amino acids, EMLA, encoded by exon 8. Current estimates suggest that *SMN2* produces 10-15% of the level of full-length protein produced by *SMN1* (Lorson et al. 2010). Complete loss of SMN is lethal in all organisms investigated to date (O'Hearn et al. 2016). Although the amount of full-length protein produced by *SMN2* is not enough to compensate for loss of *SMN1*, *SMN2* is sufficient to rescue embryonic lethality (Monani et al. 2000). SMA is therefore a disease that arises due to a hypomorphic reduction in SMN levels (Lefebvre et al. 1995). Furthermore, relative levels of the SMN protein correlate with the phenotypic severity of SMA (Coovert et al. 1997; Lefebvre et al. 1997).

Whereas a causative link between *SMN1* and SMA was established over 20 years ago, the molecular role of SMN in disease etiology remains unclear. SMN is the central component of a multimeric protein assemblage known as the SMN complex

(Matera and Wang 2014; Li et al. 2014). The best-characterized function of this complex, which is found in all tissues of metazoan organisms, is in the cytoplasmic assembly of small nuclear ribonucleoproteins (snRNPs), core components of the spliceosome (Fischer et al. 1997; Meister et al. 2001; Pellizzoni et al. 2002).

Although it is ubiquitously expressed, SMN has also been implicated in a number of tissue-specific processes related to neurons and muscles. These functions include actin dynamics (Oprea et al. 2008; Ackermann et al. 2013), axonal pathfinding (Fan and Simard 2002; McWhorter et al. 2003; Sharma et al. 2005), axonal transport of β-actin mRNP (Rossoll et al. 2003), phosphatase and tensin homolog-mediated (PTEN-mediated) protein synthesis pathways (Ning et al. 2010), translational regulation (Sanchez et al. 2013), neuromuscular junction formation and function (Chan et al. 2003; Kariya et al. 2008; Kong et al. 2009; Voigt et al. 2010), myoblast fusion (Shafey et al. 2005) and maintenance of muscle architecture (Rajendra et al. 2007; Walker et al. 2008; Bowerman et al. 2009).

Ubiquitylation pathways have been shown to regulate the stability and degradation of SMN (Chang et al. 2004; Burnett et al. 2009; Hsu et al. 2010) as well as axonal and synaptic stability (Korhonen and Lindholm 2004). In the ubiquitin proteasome system (UPS), proteins destined for degradation are tagged by linkage to ubiquitin through the action of three factors (Petroski 2008). E1 proteins activate ubiquitin and transfer it to the E2 enzyme. E2 proteins conjugate ubiquitin to their substrates. E3 proteins recognize the substrate and assist in the transfer of ubiquitin from the E2. Because E3 ligases confer substrate specificity, they are typically considered as candidates for targeted inhibition of protein degradation. Ubiquitin homeostasis is thought to be particularly important for neuromuscular pathology in SMA (Groen and Gillingwater 2015). Indeed, mouse models of SMA display widespread perturbations in UBA1 (ubiquitin-like modifier activating enzyme 1) levels (Wishart et al. 2014). Furthermore, mutations in UBA1 are known to cause X-linked infantile SMA (Ramser et al. 2008; Schmutzler et al. 2008).

Given the importance of these processes to normal development as well as neurodegenerative disease, we set out to identify and characterize novel SMN binding partners. Previously, we developed *Drosophila melanogaster* as a model system wherein the endogenous *Smn* gene is replaced with a *Flag-Smn* transgene (Praveen et

al. 2012). Although it is highly similar to human *SMN1* and *SMN2*,, the entire open reading frame of fruitfly *Smn* is contained within a single exon, and so only full-length SMN protein is expressed in *Drosophila* (Rajendra et al. 2007). When modeled in the fly, SMA-causing point mutations recapitulate the full range of phenotypic severity seen in humans (Praveen et al. 2014; Garcia et al. 2016). Using this system, we carried out proteomic profiling of Flag-purified embryonic lysates and identified the SCF^{Slmb} E3 ubiquitin ligase complex as a novel SMN interactor. Importantly, this interaction is conserved from flies to humans. We show that SCF^{Slmb} binding requires a phospho-degron motif located within the SMN self-oligomerization domain, mutation of which stabilizes SMNΔ7 and, to a lesser extent, full-length SMN. Additional studies in flies, mice and human cells elucidate a disease-relevant mechanism whereby SMN protein stability is regulated by self-oligomerization.

Results

Flag-SMN interacts with UPS (ubiquitin proteasome system) proteins

We previously generated transgenic flies that express Flag-tagged SMN proteins in an otherwise null *Smn* background (Praveen et al. 2012). To preserve endogenous expression patterns, the constructs are driven by the native promoter and flanking sequences. As described in the Methods, we intercrossed hemizygous *Flag-Smn*^{WT},*Smn*^{X7}/*Smn*^{D} animals to establish a stock wherein all of the SMN protein, including the maternal contribution, is epitope-tagged. After breeding them for >100 generations, essentially all of the animals are homozygous for the *Flag-Smn*^{WT} transgene, but second site recessive mutations are minimized due to the use of two different *Smn* null alleles. Adults from this stock display no apparent defects and have an eclosion frequency (~90%) similar to that of wild-type (Oregon-R) animals.

We collected (0-12h) embryos from *Flag-Smn*$^{WT/WT}$,*Smn*$^{X7/D}$ (SMN) and Oregon-R (Ctrl) animals and analyzed Flag-purified lysates by 'label-free' mass spectrometry. In addition to Flag-SMN, we identified SMN complex components Gemin2 and Gemin3, along with all seven of the canonical Sm-core snRNP proteins (Fig. 1A). We also identified the U7-specific Sm-like heterodimer Lsm10/11 (Pillai et al. 2003) and the Gemin5 orthologue, Rigor mortis (Gates et al. 2004). Previous studies of Schneider2 (S2) cells transfected with epitope-tagged *Smn* had identified most of the proteins listed

above as SMN binding partners in *Drosophila* (Kroiss et al. 2008). Despite bioinformatic and cell biological data indicating that Rigor mortis is part of the fruit fly SMN complex, this protein failed to co-purify with SMN in S2 cells (Kroiss et al. 2008; Cauchi et al. 2010; Guruharsha et al. 2011). On the basis of our purification data, we conclude that the conditions are effective and that Rigor mortis/Gemin5 is an integral member of the SMN complex in flies.

A detailed proteomic analysis of these flies will be presented elsewhere. However, as shown in Fig. 1B, our preliminary analysis identified 396 proteins, 114 of which were detected only in the Flag-SMN sample and not in the control. An additional 279 proteins were detected in both the Flag purification and control samples. In addition to SMN complex members, we co-purified numerous factors that are part of the ubiquitin proteasome system (UPS; Fig. 1C). Among these UPS proteins, we identified Cullin 1 (Cul1), Skp1-related A (SkpA), and supernumerary limbs (Slmb), as being highly enriched (>10 fold) in Flag-SMN samples as compared to the control. Together, these proteins comprise the SCF^{Slmb} E3 ubiquitin ligase. Cul1 forms the major structural scaffold of this horseshoe-shaped, multi-subunit complex (Zheng et al. 2002). Slmb is a F-box protein and is the substrate recognition component (Jiang and Struhl 1998). SkpA is a bridging protein essential for interaction of Cul1 with the F-box protein (Patton et al. 1998a; Patton et al. 1998b). Because of its role in substrate recognition, Slmb is likely to be the direct interacting partner of SMN within the SCF^{Slmb} complex. For this reason, we focused on Slmb for the initial validation. As shown, Slmb was easily detectable in Flag-purified eluates from embryos expressing Flag-SMN and nearly undetectable in those from control embryos (Fig. 1D). SmB and SmD3 were also easily detectable by western blot in Flag-purified embryonic lysates and were used as positive controls for known protein interaction partners of SMN. Tubulin and α-Actinin were not detected as interacting with SMN in our purification and demonstrate the specificity of the detected SMN interactions.

SCF^{Slmb} is a *bona fide* SMN interaction partner that ubiquitylates SMN

As an E3 ubiquitin ligase, the SCF^{Slmb} complex is a substrate recognition component of the ubiquitin proteasome system. As outlined in Fig. 2A, E3 ligases work with E1 and E2 proteins to ubiquitylate their targets (Fig. 2A). The interaction of SCF^{Slmb} with SMN was verified in a reciprocal co-immunoprecipitation, demonstrating that Flag-tagged SCF

components form complexes with Myc-SMN (Fig. 2B) and endogenous SMN (Fig. 2C) in S2 cells. SMN also copurified with Cul1-Flag, Flag-Slmb and to a lesser extent SkpA-Flag. Notably, when probed with anti-Myc (Fig. 2B) or anti-SMN (Fig. 2C) antibodies, Flag-Slmb reproducibly co-precipitates a ladder of four higher molecular weight SMN bands (Fig. 2B and Fig. 2C). The steps of the ladder are separated by ~8kDa, which is very close to the MW of ubiquitin. Furthermore, this ladder is not visible following immunoprecipitation by Gemin2 or any of the other SCF^{Slmb} components, which are not expected to be direct binding partners of ubiquitylated SMN (Fig. 2A). These findings suggest that Slmb associates with mono-, di-, tri-, and tetra-ubiquityltated SMN isoforms.

SCF complexes are highly conserved from flies to humans: SkpA is 77% identical to human Skp1, Cul1 is 63% identical, and Slmb is 80% identical to its human homologs, B-TrCP1 and B-TrCP2. We therefore tested the interaction of Flag-tagged *Drosophila* SCF components with endogenous human SMN in HEK 293T cells (Fig. 2D). Accordingly, human SMN was co-precipitated with Flag-Cul1 and Flag-Slmb and at lower levels following Flag-SkpA immunoprecipitation. Flag-B-TrCP1 and Flag-B-TrCP2, the two human homologs of Slmb, also copurified with endogenous human SMN in HEK 293T cells (Fig. 2E). Altogether, these data demonstrate a conserved interaction between SMN and the $SCF^{Slmb/B\text{-}TrCP}$ E3 ubiquitin ligase complex.

In order to test the functional consequences of this conserved interaction between SMN and $SCF^{Slmb/B\text{-}TrCP}$, a cell based ubiquitylation assay was performed (Fig. 2F). Protein lysate from HEK 293T cells transfected with 6xHis-Flag-ubiquitin and GFP-SMN was purified using a Ni^{2+} pull down for the tagged ubiquitin. Baseline levels of ubiquitylated GFP-SMN were detected using anti-GFP antibody. Following transfection of Flag-B-TrCP1 or Flag-B-TrCP2, the levels of ubiquitylated SMN markedly increased (Fig. 2F). Ubiquitylation levels were further increased following addition of both proteins together. These experiments demonstrate that $SCF^{Slmb/B\text{-}TrCP}$ can ubiquitylate SMN *in vivo*.

Depletion of Slmb/B-TrCP results in a modest increase in SMN levels

Given that one of the primary functions of protein ubiquitylation is to target proteins to the proteasome, we examined whether depletion of Slmb by RNA interference (RNAi) using dsRNA in S2 cells would increase SMN levels (Fig. 3A). Following Slmb RNAi,

endogenous SMN levels were modestly increased as compared to cells treated with control dsRNA. We obtained similar results using an siRNA that targets both B-TrCP1 and B-TrCP2 in HeLa cells. As shown in Fig. 3B, we detected a modest increase in levels of full-length SMN following B-TrCP RNAi, but not control RNAi. Next, we treated S2 cells with cycloheximide (CHX), in the presence or absence of dsRNA targeting Slmb, to determine whether differences in SMN levels would be exacerbated when production of new proteins was prevented (Fig. 3C). SMN protein levels were also directly targeted using dsRNA against *Smn* as a positive control for the RNAi treatment. At 6 hours post-CHX treatment there was a modest increase in full-length SMN levels following Slmb RNAi as compared to the initial timepoint (0h) or the negative control (Ctrl) RNAi (Fig. 3C). Together, these data indicate that Slmb/B-TrCP participates in the regulation of SMN protein levels.

Identification and characterization of a Slmb/B-TrCP degradation signal in SMN

Studies of numerous UPS substrates in a variety of species have revealed the presence of degradation signals (called degrons) that are required for proper E3 target recognition and binding. Slmb/B-TrCP canonically recognizes a consensus DpSGXXpS/T degron, where p indicates a phosphoryl group (Jin et al. 2005; Frescas and Pagano 2008; Fuchs et al. 2004). There are also several known variants of this motif, for example: DDGFVD, SSGYFS, TSGCSS (Kim et al. 2015). As shown in Fig. 4A, we identified a putative Slmb/B-TrCP degron (^{269}MSGYHT^{274}) in the highly conserved self-oligomerization domain (YG Box) of human SMN. Interestingly, this sequence was previously identified as part of a larger degron motif (^{268}YMSGYHTGYYMEMLA^{282}) that was thought to be created in SMNΔ7 by *SMN2* alternative splicing (Cho and Dreyfuss 2010). In particular, mutation of S270 (S201 in flies) to alanine was shown to dramatically stabilize SMNΔ7 constructs in human cells, and overexpression of SMNΔ7^{S270A} in SMN-deficient chicken DT40 cells rescued their viability (Cho and Dreyfuss 2010). However, factors responsible for specifically mediating SMNΔ7 degradation have not been identified.

In order to develop a more disease-relevant *Drosophila* system to investigate SMN YG box function, we generated a 'vertebrate-like' SMN construct, called vSmn (Fig. 4A). Transgenic flies expressing Flag-vSmn and Flag-vSmn^{S201A} in the background of an *Smn*^{X7} null mutation are fully viable (Fig. S1). In fact, the eclosion frequencies of these animals are consistently higher than those that express Flag-Smn^{WT} (Fig. S1). Additional

Smn mutant constructs were generated using the vSmn backbone, including both the full-length (e.g. vSmn^{S201A}) and truncated (e.g. vSmnΔ7A) versions of the protein (Fig. 4A). To test the effects of overall protein length and distance of the putative degron from the C-terminus, we also generated vSmn constructs that are the same length as SMNΔ7, replacing the MEMLA* (the amino acids introduced by human *SMN2* splicing) with MGLRQ*, see Fig. 4A. The S201A mutation was created in this construct as well (MGLRQ*^{S201A}). To mimic a constitutively phosphorylated state, we also introduced serine to aspartate mutations, vSmn^{S201D} and vSmnΔ7D. We transfected each of these constructs, Flag-tagged and driven by the native *Smn* promoter, into S2 cells and measured protein levels by western blotting (Fig. 4B). We note that these constructs are expressed at levels far below those of endogenous SMN protein in S2 cells; moreover, they do not affect levels of endogenous SMN (Fig. S2). As shown, the vSmn^{S201A} and vSMNΔ7A constructs exhibited increased protein levels compared to their serine containing counterparts, whereas levels of the S201D mutants were reduced, suggesting that the phospho-degron motif identified in human SMNΔ7 (Cho and Dreyfuss 2010) is also conserved in the fly protein. In addition to examining protein levels of each of these constructs in cell culture, transgenic flies expressing vSmn, vSmn^{S201A}, vSmnΔ7S, and vSmnΔ7A were created. Here again we observed that S201A mutation increased protein levels of both full-length SMN and SMNΔ7 (Fig. S3).

The MGLRQ* construct is present at levels that are similar to wild-type (vSmn) and much higher than vSmnΔ7S. Based on the crystal structures of the SMN YG box (Martin et al. 2012; Gupta et al. 2015), the presence of the MGLR insertion in *Drosophila* SMN is predicted to promote self-oligomerization (A.G.M. and G.D. Van Duyne, unpublished), thus stabilizing the protein within the SMN complex (Burnett et al. 2009). By the same logic, the relative inability of vSmnΔ7S to self-interact would be predicted to lead to its destruction. To determine whether the observed increase in SMN protein levels correlated with its ability to interact with Slmb, we co-transfected the appropriate Flag-Smn constructs with Myc-Slmb in S2 cells. Protein lysates were then Flag-immunoprecipitated and probed with anti-Myc antibody (Fig. 4C). The S201A mutation decreased binding of Slmb to both the full-length and the truncated SMN isoforms (Fig. 4C). However, the vSmnΔ7S construct co-precipitated the greatest amount of Slmb protein, despite the fact that it is present at much lower levels in the input lysate (Fig.

4C). Because SMNΔ7 is defective in self-interaction, this result suggests that the degron is more accessible to Slmb when SMN is monomeric and cannot efficiently oligomerize.

SMN self-oligomerization regulates access to the Slmb degron

To examine the connection between SMN self-oligomerization and degron accessibility more closely we took advantage of two SMA patient-derived point mutations (Y203C and G206S) that are known to destabilize the full-length protein and to decrease its self-oligomerization capacity (Praveen et al. 2014). As a control, we also employed an SMA-causing mutation (G210V) that does not disrupt SMN self-oligomerization (Praveen et al. 2014; Gupta et al. 2015). Next, we introduced the S201A degron mutation into all three of these full-length SMN constructs, transfected them into S2 cells and carried out western blotting (Figs. 4D and S2). The S201A degron mutation has a clear stabilizing effect on the G206S and Y203C constructs, as compared to the effect of S201A paired with G210V. Hence, we conclude that the Slmb degron is exposed when SMN is present predominantly as a monomer, whereas it is less accessible when the protein is able to form higher order multimers.

Mutation of the Slmb degron rescues viability and locomotion defects in SMA model flies

Next, we examined the effect of mutating the Slmb degron in the context of the full-length protein *in vivo*. We characterized adult viability, larval locomotion and SMN protein expression phenotypes of the G206S mutants in the presence or absence of the degron mutation, S201A (Fig. 5A-C). As described previously (Praveen et al. 2014), Smn^{G206S} animals express very low levels of SMN and fail to develop beyond larval stages. In contrast, flies bearing the S201A degron mutation in addition to G206S ($Smn^{6S\text{-}1A}$) express markedly increased levels of SMN protein (Fig. 5C) and a good fraction of these animals complete development (Fig. 5A). Moreover, $Smn^{6S\text{-}1A}$ larvae display significantly improved locomotor activity as compared to Smn^{G206S} or Smn^{X7} null mutants (Fig. 5B). These results strongly suggest that both the structure of the G206S mutant protein as well as its instability contribute to the organismal phenotype.

GFP-SMNΔ7 overexpression stabilizes endogenous SMN and SMNΔ7 in cultured human cells

Increased *SMN2* copy number correlates with a milder clinical phenotype in SMA patients (Oskoui et al. 2016). This phenomenon was successfully modeled in mice over a decade ago (Monani et al. 2000; Hsieh-Li et al. 2000), showing that high copy number *SMN2* transgenes fully rescue the null phenotype, whereas low copy transgenes do not. Moreover, transgenic expression of a human *SMNΔ7* cDNA construct in a low-copy *SMN2* background improves survival of this severe SMA mouse model from P5 (post-natal day 5) to P13 (Le et al. 2005). Although the truncated SMN likely retains partial functionality, the protective effect of *SMNΔ7* overexpression may not entirely be intrinsic to the protein. That is, SMNΔ7 could also act as a 'soak-off' factor, titrating the ubiquitylation machinery and stabilizing endogenous SMN. In such a scenario, the prediction would be that SMNΔ7A is less protective than SMNΔ7S because it is not a very good substrate for SCF^{Slmb}.

We therefore compared the stabilizing effects of overexpressing GFP-tagged $SMN\Delta7^{S270A}$ (SMNΔ7A) and SMNΔ7 (SMNΔ7S) on endogenous human SMN and SMNΔ7. HEK 293T cells were transfected with equivalent amounts of GFP-SMNΔ7A or -SMNΔ7S. The following day, cells were harvested after treatment with cycloheximide (CHX) for zero to ten hours. As shown in Fig. 6A, western blotting with anti-SMN showed that the SMNΔ7S construct exhibits a clear advantage over SMNΔ7A in its ability to stabilize endogenous SMN and SMNΔ7. By comparing band intensities within a given lane, we generated average intensity ratios for each time point using replicate blots (Fig. 6A, table). We then calculated a 'stabilization factor' by taking a ratio of these two ratios. As shown (Fig. 6A, graph), the protective benefit of overexpressing Δ7S vs. Δ7A at t=0 hr was roughly 3.0x for endogenous SMNΔ7 and 1.75x for full-length SMN. Thus, as predicted above, the GFP-SMNΔ7A construct was much less effective at stabilizing endogenous SMN isoforms. Because SMNΔ7 is a relatively good SCF^{Slmb} substrate, overexpression of this isoform protects full-length SMN from degradation.

As mentioned above, experiments in an SMN-deficient chicken DT40 cell line showed that expression of SMNΔ7A, but not SMNΔ7S, rescued cellular proliferation (Cho and Dreyfuss 2010). These results suggest that, when stable, SMNΔ7 is intrinsically functional. To examine SMNΔ7A functionality in a more disease-relevant cell type, control and SMA induced pluripotent stem cell (iPSC) motor neuron cultures were

transduced with lentiviral vectors expressing an mCherry control protein or SMNΔ7A (Fig. 6B). At 4 weeks post-differentiation, no statistical difference was observed between control and SMA motor neurons, however by 6 weeks, SMA motor neuron numbers had decreased significantly to approximately 7% of the total cell population (Fig. 6B). In contrast, expression of SMNΔ7A maintained motor neuron numbers to approximately the same level as the controls, and nearly two-fold greater than untreated cells (Fig. 6B). Thus expression of SMNΔ7A improves survival of human iPSCs when differentiated into motor neuron lineages.

SMNΔ7A is a protective modifier of intermediate SMA mouse phenotypes

To examine the importance of the Slmb degron in a mammalian organismal system, two previously developed SMA mouse models were utilized. As mentioned above, the 'Delta7' mouse (*Smn*$^{-/-}$*;SMN2;SMNΔ7*), is a model of severe SMA (Le et al. 2005), and affected pups usually die between P10 and P18 (Avg. P15). The '2B/–' mouse (*Smn*$^{2B/-}$) is a model of intermediate SMA (Bowerman et al. 2012; Rindt et al. 2015) and these animals survive much longer before dying, typically between P25 and P45 (Avg. P32). Adeno-associated virus serotype 9 (AAV9) was selected to deliver the SMN cDNA isoforms to these SMA mice, as this vector has previously been shown to enter and express in SMA-relevant tissues and can dramatically rescue the SMA phenotype when expressing the wild-type SMN cDNA (Foust et al. 2010; Passini et al. 2010; Valori et al. 2010; Dominguez et al. 2011; Glascock et al. 2012).

Delivery of AAV9-SMNΔ7A at P1 significantly extended survival in the intermediate 2B/– animals, resulting in 100% of the treated pups living beyond 100 days, similar to the results obtained with the full-length AAV9-SMN construct (Fig. 7A). In contrast, untreated 2B/– animals lived, on average, only 30 days. Mice treated with AAV9-SMNΔ7S survived an average of 45 days (Fig. 7A). Mice treated with AAV9-SMNΔ7D, a phosphomimetic of the wild-type serine 270 residue, have an average life span that is equivalent or slightly shorter than that of untreated 2B/– mice (Fig. 7A). These results not only highlight the specificity of the S270A mutation in conferring efficacy to SMNΔ7, but also illustrate that AAV9-mediated delivery of protein alone does not improve the phenotype.

We also analyzed the effects of SMNΔ7A expression in the severe Delta7 mouse model (Le et al. 2005). Treatment with AAV9-SMNΔ7A had only a very modest effect on

Delta7 mice, as none of the animals (treated or untreated) survived weaning (Fig. S4). These findings are similar to the results in *Drosophila*. Transgenic expression of SMNΔ7A in the *Smn* null background is not sufficient to rescue larval lethality (Fig. S3). Thus expression of SMNΔ7A provides a clear protective benefit to the viability of intermediate mice, but not to severe SMA models.

Consistent with the lifespan data, AAV9-SMNΔ7A treated 2B/– mice gained significantly more weight than either untreated or AAV-SMNΔ7S treated animals, nearly achieving the same weight as pups treated with full-length AAV-SMN (Fig. 7B). Treatment with full-length SMN cDNA resulted in animals that were clearly stronger and more mobile, consistent with the weight data (Fig. 7C). Although they did not perform as well as mice treated with full-length SMN cDNA, the SMNΔ7A treated animals retained strength and gross motor function at late time points (e.g. P100), as measured by their ability to splay their legs and maintain a hanging position using a modified tube-test, (Fig. 7C). Animals treated with AAV9-SMNΔ7D and -SMNΔ7S did not survive long enough for testing.

Discussion

Factors that recognize the putative SMNΔ7-specific degron have not been identified and the molecular mechanisms governing proteasomal access to SMN and SMNΔ7 remain unclear. In this study, we isolated factors that co-purifiy with SMN from *Drosophila* embryos that exclusively express Flag-SMN. This approach reduces potential bias towards SMN partner proteins that may be more abundant in a given tissue or cell line (Charroux et al. 1999; Meister et al. 2001; Pellizzoni et al. 2002; Kroiss et al. 2008; Trinkle-Mulcahy et al. 2008; Guruharsha et al. 2011). Here, we identify the SCF^{Slmb} E3 ubiquitin ligase complex as a novel SMN binding partner whose interaction is conserved in human. Depletion of Slmb or B-TrCP by RNAi resulted in an increase in steady-state SMN levels in *Drosophila* and human cells, respectively. Furthermore, we detected four distinct high molecular weight SMN bands following immunoprecipitation with Flag-Slmb, likely corresponding to ubiquitylated isoforms. Finally, we showed that ectopic expression of $SMN\Delta7^{S270A}$, but not SMNΔ7 or $SMN\Delta7^{S270D}$, a phosphomimetic, is a protective modifier of SMA phenotypes in animal models and human iPSC cultures.

The SCF^{Slmb} degron is exposed by *SMN2* exon skipping

A previous study posited that a phospho-degron was specifically created by exon 7 skipping and that this event represented a key aspect of the SMA disease mechanism (Cho and Dreyfuss 2010). Our identification of a putative Slmb binding site located in the C-terminal self-oligomerization domain of *Drosophila* and human SMN has allowed us to explore the molecular details of this hypothesis. The mutation of a conserved serine within the Slmb degron not only disrupted the interaction between SMN and Slmb, but also stabilized full-length SMN and SMNΔ7. Notably, the degron mutation has a greater effect on SMN levels (both full-length and Δ7) when made in the context of a protein that does not efficiently self-oligomerize. These and other findings strongly suggest that the Slmb degron is uncovered when SMN is monomeric, whereas it is less accessible when SMN forms higher-order multimers. On the basis of these results, we conclude that *SMN2* exon skipping does not *create* a potent protein degradation signal; rather, it *exposes* an existing one.

SMN targeting by multiple E2 and E3 systems

SMN degradation via the UPS is well-established (Chang et al. 2004; Burnett et al. 2009; Kwon et al. 2011). Using candidate approaches, investigators have studied other E3 ligases that have been reported to target SMN for degradation in cultured human cells (Han et al. 2016; Hsu et al. 2010; Kwon et al. 2013). Given our findings, it is therefore likely that SMN is targeted by multiple E3 ubiquitin ligases, as this regulatory paradigm has been demonstrated for a number of proteins (e.g. p53; Jain and Barton 2010). Targeting of a single protein by multiple E3 ligases is thought to provide regulatory specificity by expressing the appropriate degradation complexes only within certain tissues, subcellular compartments or developmental timeframes. Moreover, ubiquitylation does not always result in immediate destruction of the target; differential use of ubiquitin lysine linkages or chain length can alter a protein's fate (Mukhopadhyay and Riezman 2007; Ikeda and Dikic 2008; Liu and Walters 2010).

Avenues of future exploration include determination of the E2 proteins that partner with SCF^{Slmb} as well as the types of ubiquitin lysine chain linkages they add to SMN. These two questions are interconnected, as ubiquitin linkage specificity is determined by the E2 (Ye and Rape 2009). Lysine 48 (K48) linked chains typically result in degradation of the targeted protein by the 26S proteasome, whereas lysine 63 (K63)

linkage is more commonly associated with lysosomal degradation and nonproteolytic functions such as endocytosis (Tan et al. 2007; Kirkin et al. 2009; Lim and Lim 2010). Interestingly, recent work has implicated defects in endocytosis in SMA (Custer and Androphy 2014; Dimitriadi et al. 2016; Hosseinibarkooie et al. 2016). It remains to be determined how the ubiquitylation status of SMN might intersect with endocytic functions.

Does SMN function as a signaling hub?

In the Flag-SMN pulldown, we identified three E2 proteins as potential SMN interacting partners (Fig. 1C). Among them, Bendless (Ben) is particularly interesting. SMN co-purifies with Flag-Ben in *Drosophila* (Fig. S5) and physically interacts with TRAF6, an E3 ligase that functions together with Ube2N/Ubc13/Ben in human cells (Kim and Choi 2017). TRAF6 is an activator of NF-kB signaling, and its interaction with SMN is thought to inhibit this activity (Kim and Choi 2017). Notably, Ube2N/Ben heterodimerizes with Uev1a to form K63 ubiquitin linkages on target proteins (Ye and Rape 2009; van Wijk and Timmers 2010; Komander and Rape 2012; Marblestone et al. 2013; Zhang et al. 2013). Furthermore, Ben-Uev1a is involved in upstream activation of both JNK and IMD signaling in *Drosophila* (Paquette et al. 2010; Zhou et al. 2005). Previously, we and others have shown that JNK signaling is dysregulated in animal models of SMA (Garcia et al. 2013; Genabai et al. 2015; Garcia et al. 2016; Ahmad et al. 2016). Moreover, mutations in all three components of SCF^{Slmb} lead to constitutive expression of antimicrobial peptides, which are also downstream of the IMD pathway (Khush et al. 2002). Together, these findings suggest the interesting possibility of SMN functioning as a signaling hub that links the UPS to the JNK and IMD pathways, all of which have been shown to be disrupted in SMA.

Phosphorylation of the Slmb degron within SMN

As Slmb is known to recognize phospho-degrons, one of the first questions raised by our study concerns the identity of the kinase(s) responsible for phosphorylating the degron in SMN. A prime candidate is GSK3β, as this kinase recognizes a motif (SxxxS/T; Liu et al. 2007; Lee et al. 2013) that includes the degron and extends N-terminally (^{262}SxxxSxxxSxxxT^{274}, numbering as per human SMN). In support of this hypothesis, we

identified the *Drosophila* GSK3β orthologue, Shaggy (Sgg), in our SMN pulldowns (Fig. 1C). Moreover, GSK3β inhibitors as well as siRNA mediated knockdown of GSK3β were shown to increase SMN levels, primarily by stabilizing the protein (Makhortova et al. 2011; Chen et al. 2012). Finally, GSK3β is also responsible for phosphorylation of a degron in β-catenin, a well-characterized SCF^{Slmb} substrate (Liu et al. 2002). SMA mice have low levels of UBA1 (E1) ultimately leading to accumulation of β-catenin (Wishart et al. 2014). Pharmacological inhibition of β-catenin improved neuromuscular pathology in *Drosophila*, zebrafish, and mouse SMA models. β-catenin had previously been shown to regulate motor neuron differentiation and stability by affecting synaptic structure and function (Murase et al. 2002; Li et al. 2008; Ojeda et al. 2011). β-catenin also regulates motor neuron differentiation by retrograde signaling from skeletal muscle (Li et al. 2008). The connections of UBA1 and multiple SCF^{Slmb} substrates to motor neuron health thus places the UPS at the center of SMA research interest.

Concluding remarks

In summary, this study identifies conserved factors that regulate SMN stability. To our knowledge, this work represents the first time that SMN complexes have been purified in the context of an intact developing organism. Using this approach, we have demonstrated that the SCF^{Slmb} E3 ligase complex interacts with a degron embedded within the self-oligomerization domain of SMN. Our findings establish plausible connections to disease-relevant cellular processes and signaling pathways. Further, they elucidate a model whereby accessibility of the SMN phospho-degron is regulated by self-multimerization, providing an elegant mechanism for balancing functional activity with degradation.

Experimental procedures

Fly stocks and transgenes

Oregon-R was used as the wild-type control. The Smn^{X7} microdeletion allele (Chang et al. 2008) was a gift from S. Artavanis-Tsakonis (Harvard University, Cambridge, USA). This deficiency removes the promoter and the entire SMN coding region, leaving only the final 44bp of the 3' UTR. All stocks were cultured on molasses and agar at room temperature (24 ± 1°C) in half-pint bottles. The Smn transgenic constructs were injected into embryos by BestGene Inc. (Chino Hills, CA) as described in Praveen et al. 2014. In short, a ~3kb fragment containing the entire *Smn* coding region was cloned from the *Drosophila* genome into the pAttB vector (Bischof et al. 2007). A 3X FLAG tag was inserted immediately downstream of the start codon of dSMN. Point mutations were introduced into this construct using Q5 (NEB) site-directed mutagenesis according to manufacturer's instructions. The basal Smn construct used, vSmn, contained three single amino acid changes and the addition of the MGLR motif to make fruitfly Smn more similar to the evolutionarily conserved vertebrate Smn. Subsequently generated constructs used vSmn as a template and consist of the amino acid changes detailed in Figure 4. Y203C, G206S, and G210V were previously published in Praveen et al. 2014.

Drosophila embryo protein lysate and mass spectrometry

0-12h Drosophila embryos were collected from Oregon-R control and Flag-SMN flies, dechorionated, flash frozen, and stored at -80C. Embryos (approx. 1gr) were then homogenized on ice with a Potter tissue grinder in 5 mL of lysis buffer containing 100mM potassium acetate, 30mM HEPES-KOH at pH 7.4, 2mM magnesium acetate, 5mM dithiothreitol (DTT) and protease inhibitor cocktail. Lysates were centrifuged twice at 20000 rpm for 20min at 4C and dialyzed for 5h at 4C in Buffer D (HEPES 20mM pH 7.9, 100mM KCl, 2.5 mM $MgCl_2$, 20% glycerol, 0.5 mM DTT, PMSF 0.2 mM). Lysates were clarified again by centrifugation at 20000 rpm for 20 min at 4C. Lysates were flash frozen using liquid nitrogen and stored at -80C before use. Lysates were then thawed on ice, centrifuged at 20000 rpm for 20 min at 4C and incubated with rotation with 100 μL of EZview Red Anti-FLAG M2 affinity gel (Sigma) for 2h at 4C. Beads were washed a total of six times using buffer with KCl concentrations ranging from 100mM to 250mM with rotation for 1 min at 4C in between each wash. Finally, Flag proteins were eluted 3 consecutive times with one bed volume of elution buffer (Tris 20mM pH 8, 100 mM KCl,

10% glycerol, 0.5 mM DTT, PMSF 0.2 mM) containing 250ug/mL 3XFLAG peptide (sigma). The entire eluate was used for mass spectrometry analysis on an Orbitrap Velos instrument, fitted with a Thermo Easy-spray 50cm column.

Tissue culture and transfections

S2 cell lines were obtained from the Drosophila Genome Resource Center (Bloomington, IL). S2 cells were maintained in SF900 SFM (Gibco) supplemented with 1% penicillin/streptomycin and filter sterilized. Cells were removed from the flask using a cell scraper and passaged to maintain a density of approximately 10^6-10^7 cells/mL. S2 cells were transferred to filter sterilized SF900 SFM (Gibco) without antibiotics prior to transfection with Cellfectin II (Invitrogen). Transfections were performed according to Cellfectin II protocol in a final volume of 4 mL in a T-25 flask containing 10^7 cells that were plated one hour before transfection. The total amount of DNA used in transfections was 2.5ug. Human embryonic kidney HEK-293T and HeLa cells were maintained at 37C with 5% CO_2 in DMEM (Gibco) supplemented with 10% FBS and 1% penicillin/streptomycin (Gibco). $1x10^6$ - $2x10^6$ cells were plated in T-25 flasks and transiently transfected with 1-2ug of plasmid DNA per flask using Lipofectamine (Invitrogen) or FuGENE HD transfection reagent (Roche Applied Science, Indianapolis, IN) according to the manufacturer's protocol. Cells were harvested 24-72 h posttransfection.

For siRNA transections, HeLa cells were plated subconfluently in T-25 flasks and transfected with 10nm of siRNA (Gift from Mike Emanuele lab) and 17uL Lipofectamine RNAi MAX (Invitrogen) in 5mL total media according to manufacturers instructions. After 48h of transfection cells were harvested. For RNAi in S2 cells using dsRNA, 10^7 cells were plated in each well of a 6-well plate in 1 mL of media. Cells were treated ~ every 24h with 10ug/mL dsRNA targeted against Slmb, Oskar, or Gaussia Luciferaese (as controls) as described in Rogers and Rogers 2008.

***In vivo* ubiquitylation assay**

The *in vivo* ubiquitylation assay was performed as described previously (Choudhury et al. 2016). Briefly, HEK-293T cells were transfected as indicated in 10 cm dishes using Lipofectamine2000 (Thermo Fisher Scientific). The day after, cells were treated with 20 μM of MG132 for 4 hours and then harvested in PBS. 80% of the cell suspension was

lysed in 6M Guanidine-HCl containing buffer and used to pull down His-Ubiquitinated proteins on Ni2+-NTA beads, while the remaining 20% was used to prepare inputs. Ni2+ pull down eluates and inputs were separated through SDS-PAGE and analyzed by western blot.

Cycloheximide treatment

Following RNAi treatment, S2 cells were pooled, centrifuged and resuspended in fresh media. 1/3 of these cells were frozen and taken as the 0h timepoint. The remainders of the cells were replated in 6 well plates. 100ug/mL cycloheximide (CHX) was added to each sample, and cells were harvested at 2 and 6 hours following treatment.

Immunoprecipitation

Clarified cell lysates were precleared with immune-globulin G (IgG) agarose beads for 1h at 4C and again precleared overnight at 4C. The precleared lysates were then incubated with Anti-FLAG antibody crosslinked to agarose beads (EZview Red Anti-FLAG M2 affinity gel, Sigma) for 2h at 4C with rotation. The beads were washed with lysis buffer or modified lysis buffer six times and boiled in SDS gel-loading buffer. Eluted proteins were run on an SDS-PAGE for western blotting.

Antibodies and Western blotting

Larval and adult lysates were prepared by crushing the animals in lysis buffer (50mM Tris-HCl, pH 7.5, 150 mM NaCl, 1mM EDTA, 1% NP-40) with 1X (adults) or 10x (larvae) protease inhibitor cocktail (Invitrogen) and clearing the lysate by centrifugation at 13,000 RPM for 10 min at 4ºC. S2 cell lysates were prepared by suspending cells in lysis buffer (50mM Tris-HCl, pH 7.5, 150 mM NaCl, 1mM EDTA, 1% NP-40) with 10% glycerol and 1x protease inhibitor cocktail (Invitrogen) and disrupting cell membranes by pulling the suspension through a 25 gauge needle (Becton Dickinson). The lysate was then cleared by centrifugation at 13,000 RPM for 10 min at 4ºC. Human cells (293Ts and HeLas) were first gently washed in ice-cold 1X PBS, then collected in ice-cold 1X PBS by scraping. Cells were pelleted by spinning at 1000 rpm for 5 min. The supernatant was removed and cells were resuspended in ice cold lysis buffer (50mM Tris-HCl, pH 7.5, 150 mM NaCl, 1mM EDTA, 1% NP-40) and allowed to lyse on ice for 30 min. After lysing, the lysate was cleared by centrifuging the cells for 10 min at 13000 at 4C.

Western blotting on lysates was performed using standard protocols. Rabbit anti-dSMN serum was generated by injecting rabbits with purified full-length dSMN protein (Pacific Immunology Corp, CA), and was subsequently affinity purified. For Western blotting, dilutions of 1 in 2,500 for the affinity purified anti-dSMN, 1 in 20,000 (fly) or 1 in 5,000 (human) for anti-α tubulin (Sigma), 1 in 10,000 for monoclonal anti-Flag (Sigma), 1 in 1,000 for anti-Slmb (gift from Greg Rogers), 1 in 2,500 for anti-human SMN (BD Biosciences), 1 in 1,000 for anti-B-TrCP (gift from MB Major lab), and 1 in 10,000 for polyclonal anti-Myc (Santa Cruz) were used.

Larval locomotion

Smn control and mutant larvae (73-77 hours post egg-laying) were placed on a 1.5% agarose molasses tray five at a time. The tray was then placed in a box with a camera and the larvae were recorded moving freely for 60 seconds. Each set of larvae was recorded three times, and one video was chosen for analysis based on video quality. The videos were then converted to AVI files and analyzed using the wrMTrck plug-in of the Fiji software. The "Body Lengths per Second" was calculated in wrMTrck by dividing the track length by half the perimeter and time (seconds). P-values were generated using a multiple comparison ANOVA.

SMA Mouse Models

Two previously developed SMA mouse models were utilized. The 'Delta7' mouse ($Smn^{-/-}$;*SMN2;SMNΔ7*), is a model of severe SMA (Le et al. 2005). The '2B/–' mouse ($Smn^{2B/-}$) is a model of intermediate SMA (Bowerman et al. 2012; Rindt et al. 2015). Adeno-associated virus serotype 9 (AAV9) delivered SMN cDNA isoforms to these SMA mice, as previously described (Foust et al. 2010; Passini et al. 2010; Valori et al. 2010; Dominguez et al. 2011; Glascock et al. 2012). Gross motor function was measured using a modified tube-test which tests the ability of mice to splay their legs and maintain a hanging position.

Human iPSC Cell culture

Human iPSCs from two independent unaffected control and two SMA patient lines were grown as pluripotent colonies on Matrigel substrate (Corning) in Nutristem medium (Stemgent). Colonies were then lifted using 1mg/ml Dispase (Gibco) and maintained as

floating spheres of neural progenitor cells in the neural progenitor growth medium Stemline (Sigma) supplemented with 100ng/ml human basic fibroblast growth factor (FGF-2, Miltenyi), 100ng/ml epidermal growth factor (EGF, Miltenyi), and 5μg/ml heparin (Sigma-Aldrich) in ultra-low attachment flasks. Aggregates were passaged using a manual chopping technique as previously described (Svendsen et al. 1998; Ebert et al. 2013). To induce motor neuron differentiation, neural progenitor cells were cultured in neural induction medium (1:1 DMEM/F12 (Gibco), 1x N2 Supplement (Gibco), 5μg/mL Heparin (Sigma), 1x Non-Essential Amino Acids (Gibco), and 1x Antibiotic-Antimycotic (Gibco)) plus 0.1μM all-trans retinoic acid (RA) for two weeks; 1μM Purmorphamine (PMN, Stemgent) was added during the second week. Spheres were then dissociated with TrypLE Express (Gibco) and plated onto Matrigel-coated 12mm coverslips in NIM plus 1μM RA, 1μM PMN, 1x B27 Supplement (Gibco), 200ng/mL Ascorbic Acid (Sigma), 1μM cAMP (Sigma), 10ng/mL BDNF (Peprotech), 10ng/mL GDNF (Peprotech)). One week post-plating, cells were infected with lentiviral vectors (MOI = 5) expressing mCherry alone or SMN S270A-IRES-mCherry. Transgenes in both viruses were under the control of the EF1α promoter. Uninfected cells served as controls. Cells were analyzed at 1 and 3 weeks post-infections, which was 4 and 6 weeks of total differentiation (Ebert et al. 2009; Sareen et al. 2013).

Immunocytochemistry

Coverslips were fixed in 4% paraformaldehyde (Electron Microscopy Sciences) for 20 minutes at room temperature and rinsed with PBS. Cells were blocked with 5% Normal Donkey Serum (Millipore) and permeabilized in 0.2% TritonX-100 (Sigma) for 30 minutes at room temperature. Cells were then incubated in primary antibody solution for 1 hour, rinsed with PBS, and incubated in secondary antibody solution for 1 hour at room temperature. Finally, nuclei were labeled with Hoechst nuclear stain (Sigma) to label DNA and mounted onto glass slides using FluoroMount medium (SouthernBiotech). Primary antibodies used were mouse anti-SMI-32 (Covance SMI-32R, 1:1000) and rabbit anti-mCherry (ThermoFisher, 1:1000). Secondary antibodies used were donkey anti-rabbit Cy3 (Jackson Immunoresearch 711-165-152) and donkey anti-mouse AF488 (Invitrogen A21202).

Immunocytochemical Analysis

Images were acquired from five random fields per coverslip using an inverted fluorescent microscope (Nikon) and NIS Elements software. Images were blinded and manually analyzed for antigen specificity with NIS Elements software.

Acknowledgements

This work was supported by NIGMS R01 GM118636 (to A.G.M.). K.M.G. was supported by graduate research fellowship DGE-1144081 from the NSF. Work in the Wagner lab (D.B and E.J.W.) was supported by the Welch Foundation (H1889). We also thank the Peifer, Major, and Rogers laboratories for reagents, advice and expertise.

Figure Legends

Figure 1: Flag-SMN immunopurified lysates contain known protein interaction partners and ubiquitin proteasome system (UPS) proteins. ***A.*** Lysates from Oregon-R control (Ctrl) *Drosophila* embryos and embryos expressing only transgenic Flag-SMN (SMN) were Flag-immunopurified and protein eluates were separated by gel electrophoresis and silver stained. Band identities predicted by size using information from panels C and D. ***B.*** Direct mass spectrometric analysis of the eluates (which were not gel purified) identified a total of 396 proteins, 114 of which were detected only in SMN sample and 279 of which were detected in both SMN and Ctrl samples. ***C***. Flag-purified eluates were analyzed by 'label-free' mass spectrometry. Numerous proteins that copurify with Flag-SMN are part of the ubiquitin proteasome system (UPS). Of these UPS proteins, Cullin 1 (Cul 1), SkpA, and supernumerary limbs (Slmb), were highly enriched (at least 10 fold) in the SMN sample as compared to Ctrl. ***D.*** Western blot analysis of Flag-purified eluates was used to further validate the presence or absence of SMN interaction partners. Flag-SMN was successfully purified from SMN embryos, but was undetectable in the control. As positive controls for known protein interaction partners of SMN, SmB and SmD3 were also easily detectable by western blotting using anti-Sm antibodies. The presence of Slmb was verified using anti-Slmb. α-Actinin and Tubulin were not enriched in our purification and are used as negative controls to demonstrate specificity.

Figure 2. Conserved interaction between SMN and the $SCF^{Slmb/B\text{-}TrCP}$ E3 ubiquitin ligase results in ubiquitylation of SMN. ***A.*** E3 ligases work with E1 and E2 proteins to

ubiquitylate their targets. The $SCF^{Slmb/B\text{-}TrCP}$ E3 ubiquitin ligase is made up of three proteins: Cul1, SkpA, and Slmb. The E3 ubiquitin ligase is the substrate recognition component of the ubiquitin proteasome system. ***B.*** The interactions of SMN with Cullin1, SkpA, and Slmb were examined in a co-immunoprecipitation demonstrating Flag-tagged SCF components interact with Myc-SMN in Drosophila S2 cells. SMN was detected following immunoprecipitation of Cul1-Flag and Flag-Slmb. When probed with anti-Myc antibody, Flag-Slmb co-precipitates a ladder of four higher molecular weight SMN bands separated by ~8kDa. ***C***. Following Cul1-Flag and Flag-Slmb immunoprecipitation from Drosophila S2 cell lysates, western analysis using anti-SMN antibody for endogenous SMN was carried out. A protein ladder, with each band separated by ~8kDa, was detected following Flag-Slmb purification. * is a non-specific band detected by the Drosophila SMN antibody. ***D.*** The interaction of Flag-tagged Drosophila SCF components with endogenous human SMN was tested in in HEK 293T cells. Human SMN was detected at high levels following immunoprecipitation of Drosophila Flag-Cul1 and Flag-Slmb and detected at a lower level following Drosophila Flag-SkpA immunoprecipitation. ***E.*** Flag-tagged versions of the human homologs of Slmb, Flag-B-TrCP1 and Flag-B-TrCP2, interact with endogenous human SMN in HEK 293T cells demonstrated by Flag-immunopurification followed by immunodetection of SMN. ***F.*** Protein lysate from HEK 293T cells transfected with 6xHis-Flag-ubiquitin (6HF-Ub) and GFP-SMN was purified using a Ni^{2+} pull down for the tagged ubiquitin. Baseline levels of ubiquitylated GFP-SMN were detected using anti-GFP antibody. Following transfection of Flag-B-TrCP1 or Flag-B-TrCP2, the levels of ubiquitylated SMN markedly increased. Ubiquitylation levels were further increased following addition of both proteins together. In the input, GFP-SMN was detected using anti-GFP antibody, Flag-B-TrCP1 and Flag-B-TrCP2 were detected using anti-Flag antibody, and GAPDH was detected by anti-GAPDH antibody. In the Ni^{2+} pull down, ubiquitylated GFP-SMN was detected using anti-GFP antibody and 6HF-Ub was detected using anti-Flag antibody to verify successful pull down of tagged ubiquitin.

Figure 3. Depletion of Slmb/B-TrCP results in an increase of SMN levels. ***A.*** Depletion of Slmb using 10 day (10d) treatment with dsRNA in *Drosophila* S2 cells resulted in modestly increased SMN levels. Following Slmb RNAi, full-length SMN levels were increased as compared to cells treated with control dsRNA against Gaussia Luciferase,

which is not expressed in S2 cells. ***B.*** The effect of B-TrCP depletion on SMN levels in human cells was tested using siRNA that targets both B-TrCP1 and B-TrCP2 in HeLa cells. We detected a modest increase in levels of full-length endogenous SMN after B-TrCP RNAi but not control (scramble) RNAi. ***C***. *Drosophila* S2 cells were treated with cycloheximide (CHX), an inhibitor of protein synthesis, following Slmb depletion following a 3d dsRNA treatment to test whether differences in protein levels would be exacerbated when the production of new protein was prevented. SMN protein levels were also directly targeted using dsRNA against *Smn* as a positive control for the RNAi treatment. As a negative control (Ctrl), dsRNA against *oskar*, which is not expressed in S2 cells, was used. Protein was collected at 0, 2, and 6 hours post CHX treatment. At 6 hours post-CHX treatment there is a modest increase in full-length SMN levels following *Slmb* RNAi as compared to the initial timepoint (0h) and as compared to control RNAi treatment.

Figure 4: Identification and mutation of a putative Slmb/B-TrCP phospho-degron ***A***. Identification of a conserved putative Slmb phospho-degron (DpSGXXpS/T motif variant) in the C-terminal self-oligomerization domain (YG Box) of SMN. The amino acid sequence of Smn from a variety of vertebrates is shown to illustrate conservation of this motif and rationale for the amino acid changes. Full-length human SMN is labeled as "Human" and the truncated isoform is labeled "hSMNΔ7". Endogenous *Drosophila melanogaster* Smn is labeled "Fruitfly". To generate a more vertebrate-like SMN, key amino acids in Drosophila SMN were changed to amino acids conserved in vertebrates. Using this SMN backbone, a serine to alanine mutation was made in the putative degron in both full-length ($vSMN^{S201A}$) and truncated SMNΔ7 (vSMNΔ7A). An additional SMN construct that is the same length as SMNΔ7, but has the amino acid sequence GLRQ (the next amino acids in the sequence) rather than EMLA (the amino acids introduced by mis-splicing of *SMN2*) was made. The same serine to alanine mutation was made in this construct as well (MGLRQ* and $MGLRQ^{*S201A}$). Finally, to mimic a phosphorylated serine the full-length SMN construct ($vSmn^{S201D}$) and truncated SMN (vSmnΔ7D) were made. ***B.*** Western blotting was used to determine protein levels of each of these SMN constructs, with expression driven by the endogenous promoter, in Drosophila S2 cells. Both the vSMN and vSMNΔ7S proteins show increased levels when the serine is mutated to an alanine, indicating disruption of the normal degradation of SMN. Additionally, MGLRQ* protein is present at higher levels than is vSMNΔ7S and protein

levels do not change when the serine is mutated to an alanine. Normalized fold change as compared to vSmn levels is indicated at the bottom. *p<0.05, **p<0.01 n=3. ***C.*** Flag-tagged SMN constructs were co-transfected with Myc-Slmb in Drosophila S2 cells. Protein lysates were Flag-immunoprecipitated and probed with anti-Myc antibody to detect SMN-Slmb interaction. In both full-length SMN (vSMN) and truncated SMN (vSMNΔ7), serine to alanine mutation decreased interaction of Slmb with SMN. Truncated SMN (vSMNΔ7) showed a dramatically increased interaction with Slmb as compared to full-length SMN (vSMN), despite the fact it is present at lower levels. ***D***. Full-length SMN constructs containing point mutations known to decrease self-oligomerization (Smn^{Y203C} and Smn^{G206S}) and a mutation that does not disrupt self-oligomerization in the fly (Smn^{G210V}) with and without the serine to alanine mutation were transfected in Drosophila S2 cells. The constructs containing the serine to alanine mutation are as follows: Smn^{Y203C}->Smn^{3C-1A}, Smn^{G206S}->Smn^{6S-1A}, Smn^{G210V}->Smn^{10V-1A}. The serine to alanine mutation has a stabilizing effect on SMN mutants with poor self-oligomerization capability. *p<0.05, n=3.

Figure 5: Mutation of the Slmb degron rescues defects in SMA model flies. ***A.*** Viability analysis of an SMA point mutation (G206S) in the presence and absence of the degron mutation, S201A. Flies with the following genotypes were analyzed in this experiment: Oregon-R (Ctrl), *Flag-Smn*^{WT},*Smn*^{X7}/*Smn*^{X7} (Smn^{WT}), *Flag-Smn*^{G206S},*Smn*^{X7}/*Smn*^{X7} (Smn^{G206S}), *Flag-Smn*^{G206,S201A},*Smn*^{X7}/*Smn*^{X7} (Smn^{6S-1A}) or *Smn*^{X7}/*Smn*^{X7} (Smn^{X7}). The data for each genotype are expressed as a fraction of pupae or adults over the total number of starting larvae, n=200. Expression of the WT transgene (*Smn*^{WT}) shows robust rescue of the null (*Smn*^{X7}) phenotype (~68% adults). *Smn*^{G206S} is a larval lethal mutation. In two independent recombinant lines of *Smn*$^{6S-1A}$ (*Smn*$^{6S-1A}$*1* and *Smn*$^{6S-1A}$*2*) a fraction of the larvae complete development to become adults. ***B.*** Locomotor ability of early 3rd instar larvae was determined by tracking their movement for one minute and then calculating the velocity. To account for potential differences in larval size, speed is expressed as average body lengths per second moved. Genotypes are as in panel A. *Smn*^{G206S} larvae move similarly to null animals. The motility of *Smn*$^{6S-1A}$*1* and *Smn*$^{6S-1A}$*2* larvae is not different from Ctrl or *Smn*^{WT} larvae. ***p<0.001, n=50 to 60 larvae. ***C.*** Larval protein levels were examined by western blotting; genotypes as in panel A. Lysates from hemizygous mutant lines were probed with anti-Flag or anti-SMN antibodies as

indicated. The slower migrating bands represent the Flag-tagged transgenic proteins and the faster migrating band corresponds to endogenous SMN, which is present only in the Ctrl (note Oregon-R has two copies *Smn* whereas the transgenics have only one). *Smn*^{G206S} has very low levels of SMN protein. Flies bearing the S201A degron mutation in addition to G206S (*Smn*$^{6S\text{-}1A}$) express markedly increased levels of SMN protein.

Figure 6: Stabilization of endogenous SMN and SMNΔ7 in cultured human cells. ***A***. HEK 293T cells were transfected with equivalent amounts of GFP-SMNΔ7A or -SMNΔ7S. The following day, cells were harvested after treatment with cycloheximide (CHX) for zero to ten hours. Western blotting with anti-SMN showed that SMNΔ7S stabilizes endogenous SMN and SMNΔ7 to a greater extent than SMNΔ7A. By comparing band intensities within a given lane, we generated average intensity ratios for each time point using replicate blots. We then calculated a 'stabilization factor' by taking a ratio of these two ratios. The protective benefit of overexpressing Δ7S vs. Δ7A at t=0 hr was roughly 3.0x for endogenous SMNΔ7 and 1.75x for full-length SMN. ***B.*** SMNΔ7A (S270A) expression protects SMA iPSC-derived motor neurons. Control motor neurons were left untreated or transduced with a lentiviral vector expressing an mCherry control. SMA motor neurons were left untreated, transduced with a lentiviral vector expressing an mCherry control, or a lentiviral vector expressing SMNΔ7A (S270A). At 4 weeks of differentiation, there was no difference in motor neuron survival between control and SMA iPSC motor neuron cultures in any of the treatment groups. However, at 6 weeks, SMI-32 positive motor neurons showed selective loss in SMA iPSC motor neuron cultures in the untreated and lenti-mCherry groups compared to control iPSC motor neuron cultures. In contrast, lenti-SMNΔ7A expression fully protects SMA iPSC-derived motor neurons. Representative images of control and SMA iPSC-derived motor neurons labeled with SMI-32 (green) and mCherry (red). Nuclei are stained with DAPI and shown in blue. *$p<0.05$ by ANOVA. NS = not significant. n=3

Figure 7: SMNΔ7A is a protective modifier of intermediate SMA phenotypes in mice. ***A***. Mouse genotypes include control unaffected *Smn*$^{2B/+}$ mice, which have a wild-type *Smn* allele, *Smn*$^{2B/-}$ (2B/–) mice treated with scAAV9 expressing different versions of SMN, and untreated 2B/– mice, which are an intermediate mouse model of SMA. 1e11 denotes the viral dose. scAAV9-SMN expresses full-length SMN, scAAV9-SMNΔ7

expresses truncated SMN, scAAV9-SMNΔ7^{S270A} expresses truncated SMN with the S to A change in the degron, and scAAV9-SMNΔ7^{S270D} expresses truncated SMN with a phosphomimic in the degron. Delivery of AAV9-SMNΔ7A at P1 significantly extended survival in the intermediate 2B/– animals, resulting in 100% of the treated pups living beyond 100 days, similar to the results obtained with the full-length AAV9-SMN construct. Untreated 2B/– animals lived, on average, only 30 days. Mice treated with AAV9-SMNΔ7S survived an average of 45 days. Mice treated with AAV9 expressing SMNΔ7D had an average life span equivalent or slightly worse than that of untreated 2B/– mice. ***B.*** Average weight (measured over time) of the animals used in panel A. AAV9-SMNΔ7A treated mice also gained significantly more weight than either untreated or AAV-SMNΔ7S treated animals, nearly achieving the same weight as 2B/– pups treated with full-length SMN cDNA. ***C.*** Mouse genotypes include control unaffected *Smn*$^{2B/+}$ mice, which carry a wild-type *Smn* allele, and 2B/– mice treated with scAAV9 expressing different versions of SMN. scAAV9-SMN expresses full-length SMN and scAAV9-SMNΔ7^{S270A} expresses truncated SMN with the S to A change in the degron. AAV-SMNΔ7A treated animals retained their improved strength and gross motor functions at late time points (P100), as measured by their ability to splay their legs and maintain a hanging position using a modified tube-test.

References

Ackermann B, Kröber S, Torres-Benito L, Borgmann A, Peters M, Hosseini Barkooie SM, Tejero R, Jakubik M, Schreml J, Milbradt J, et al. 2013. Plastin 3 ameliorates spinal muscular atrophy via delayed axon pruning and improves neuromuscular junction functionality. *Hum Mol Genet* **22**: 1328–1347.

Ahmad S, Bhatia K, Kannan A, Gangwani L. 2016. Molecular Mechanisms of Neurodegeneration in Spinal Muscular Atrophy. *J Exp Neurosci* **10**: 39–49.

Bischof J, Maeda RK, Hediger M, Karch F, Basler K. 2007. An optimized transgenesis system for Drosophila using germ-line-specific phiC31 integrases. *Proc Natl Acad Sci USA* **104**: 3312–3317.

Bocca SN, Muzzopappa M, Silberstein S, Wappner P. 2001. Occurrence of a putative SCF ubiquitin ligase complex in Drosophila. *Biochem Biophys Res Commun* **286**: 357–364.

Bowerman M, Anderson CL, Beauvais A, Boyl PP, Witke W, Kothary R. 2009. SMN, profilin IIa and plastin 3: A link between the deregulation of actin dynamics and SMA pathogenesis. *Mol Cell Neurosci* **42**: 66–74.

Bowerman M, Murray LM, Beauvais A, Pinheiro B, Kothary R. 2012. A critical smn threshold in mice dictates onset of an intermediate spinal muscular atrophy phenotype associated with a distinct neuromuscular junction pathology. *Neuromuscul Disord* **22**: 263–276.

Burghes Arthur HM, Beattie Christine E. 2009. Spinal muscular atrophy: why do low levels of survival motor neuron protein make motor neurons sick? *Nat Rev Neurosci* **10**: 597–609.

Burnett BG, Muñoz E, Tandon A, Kwon DY, Sumner CJ, Fischbeck KH. 2009. Regulation of SMN protein stability. *Mol Cell Biol* **29**: 1107–1115.

Cauchi RJ, Sanchez-Pulido L, Liu J-L. 2010. Drosophila SMN complex proteins Gemin2, Gemin3, and Gemin5 are components of U bodies. *Exp Cell Res* **316**: 2354–2364.

Chan YB, Miguel-Aliaga I, Franks C, Thomas N, Trülzsch B, Sattelle DB, Davies KE, van den Heuvel M. 2003. Neuromuscular defects in a Drosophila survival motor neuron gene mutant. *Hum Mol Genet* **12**: 1367–1376.

Chang HCH, Dimlich DN, Yokokura T, Mukherjee A, Kankel MW, Sen A, Sridhar V, Fulga TA, Hart AC, Van Vactor D, et al. 2008. Modeling spinal muscular atrophy in Drosophila. *PLoS One* **3**: e3209.

Chang HC, Hung WC, Chuang YJ, Jong YJ. 2004. Degradation of survival motor neuron (SMN) protein is mediated via the ubiquitin/proteasome pathway. *Neurochem Int* **45**: 1107–1112.

Charroux B, Pellizzoni L, Perkinson RA, Shevchenko A, Mann M, Dreyfuss G. 1999. Gemin3: A novel DEAD box protein that interacts with SMN, the spinal muscular atrophy gene product, and is a component of gems. *J Cell Biol* **147**: 1181–1193.

Chen PC, Gaisina IN, El-Khodor BF, Ramboz S, Makhortova NR, Rubin LL, Kozikowski AP. 2012. Identification of a maleimide-based glycogen synthase kinase-3 (GSK-3) inhibitor, BIP-135, that prolongs the median survival time of Δ7 SMA KO mouse model of spinal muscular atrophy. *ACS Chem Neurosci* **3**: 5–11.

Cho S, Dreyfuss G. 2010. A degron created by SMN2 exon 7 skipping is a principal contributor to spinal muscular atrophy severity. *Genes Dev* **24**: 438–442.

Choudhury R, Bonacci T, Arceci A, Decaprio JA, Burke DJ, Emanuele MJ, Choudhury R, Bonacci T, Arceci A, Lahiri D, et al. 2016. APC/C and SCF Cyclin F Constitute a Reciprocal Feedback Circuit Controlling S-Phase Entry. *Cell Reports* **16**: 3359–3372.

Coovert DD, Le TT, McAndrew PE, Strasswimmer J, Crawford TO, Mendell JR, Coulson SE, Androphy EJ, Prior TW, Burghes AHM. 1997. The survival motor neuron protein in spinal muscular atrophy. *Hum Mol Genet* **6**: 1205–1214.

Crawford TO, Pardo CA. 1996. The Neurobiology of Childhood Spinal Muscular Atrophy. *Neurobiol Dis* **3**: 97–110.

Custer SK, Androphy EJ. 2014. Autophagy dysregulation in cell culture and animals models of spinal muscular atrophy. *Mol Cell Neurosci* **61**: 133–140.

Dimitriadi M, Derdowski A, Kalloo G, Maginnis MS, Bliska B, Sorkaç A, Q Nguyen KC, Cook SJ, Poulogiannis G, Atwood WJ, et al. 2016. Decreased function of survival motor neuron protein impairs endocytic pathways. *Proc Natl Acad Sci USA* 4377–4386.

Dominguez E, Marais T, Chatauret N, Benkhelifa-Ziyyat S, Duque S, Ravassard P, Carcenac R, Astord S, de Moura AP, Voit T, et al. 2011. Intravenous scAAV9 delivery of a codon-optimized SMN1 sequence rescues SMA mice. *Hum Mol Genet* **20**: 681–693.

Ebert AD, Yu J, Rose FF, Mattis VB, Lorson CL, Thomson JA, Svendsen CN. 2009. Induced pluripotent stem cells from a spinal muscular atrophy patient. *Nature* **457**: 277–280.

Ebert AD, Shelley BC, Hurley AM, Onorati M, Castiglioni V, Patitucci TN, Svendsen SP, Mattis VB, McGivern J V., Schwab AJ, et al. 2013. EZ spheres: A stable and expandable culture system for the generation of pre-rosette multipotent stem cells from human ESCs and iPSCs. *Stem Cell Res* **10**: 417–427.

Fan L, Simard LR. 2002. Survival motor neuron (SMN) protein: role in neurite outgrowth and neuromuscular maturation during neuronal differentiation and development. *Hum Mol Genet* **11**: 1605–1614.

Fischer U, Liu Q, Dreyfuss G. 1997. The SMN-SIP1 Complex Has an Essential Role in Spliceosomal snRNP Biogenesis. *Cell* **90**: 1023–1029.

Foust KD, Wang X, McGovern VL, Braun L, Bevan AK, Haidet AM, Le TT, Morales PR, Rich MM, Burghes AHM, et al. 2010. Rescue of the spinal muscular atrophy

phenotype in a mouse model by early postnatal delivery of SMN. *Nat Biotechnol* **28**: 271–274.

Frescas D, Pagano M. 2008. Deregulated proteolysis by the F-box proteins SKP2 and B-TrCP: tipping the scales of cancer. *Nat Rev Cancer* **8**: 438–449.

Fuchs SY, Spiegelman VS, Kumar KGS. 2004. The many faces of B-TrCP E3 ubiquitin ligases: reflections in the magic mirror of cancer. *Oncogene* **23**: 2028–2036.

Garcia EL, Lu Z, Meers MP, Praveen K, Matera AG. 2013. Developmental arrest of Drosophila survival motor neuron (Smn) mutants accounts for differences in expression of minor intron-containing genes. *RNA* **19**: 1510–1516.

Garcia EL, Wen Y, Praveen K, Matera AG. 2016. Transcriptomic comparison of Drosophila snRNP biogenesis mutants reveals mutant-specific changes in pre-mRNA processing: implications for spinal muscular atrophy. *RNA* 1–13.

Gates J, Lam G, Ortiz J, Losson R, Thummel CS. 2004. rigor mortis encodes a novel nuclear receptor interacting protein required for ecdysone signaling during Drosophila larval development. *Development* **131**: 25–36.

Genabai NK, Ahmad S, Zhang Z, Jiang X, Gabaldon CA, Gangwani L. 2015. Genetic inhibition of JNK3 ameliorates spinal muscular atrophy. *Hum Mol Genet* **24**: 6986–7004.

Glascock JJ, Shababi M, Wetz MJ, Krogman MM, Lorson CL. 2012. Direct central nervous system delivery provides enhanced protection following vector mediated gene replacement in a severe model of Spinal Muscular Atrophy. *Biochem Biophys Res Commun* **417**: 376–381.

Groen EJN, Gillingwater TH. 2015. UBA1: At the Crossroads of Ubiquitin Homeostasis and Neurodegeneration. *Trends Mol Med* **21**: 622–632.

Gupta K, Martin R, Sharp R, Sarachan KL, Ninan NS, Van Duyne GD. 2015. Oligomeric Properties of Survival Motor Neuron.Gemin2 Complexes. *J Biol Chem* **290**: 20185–20199.

Guruharsha KG, Rual J-F, Zhai B, Mintseris J, Vaidya P, Vaidya N, Beekman C, Wong C, Rhee DY, Cenaj O, et al. 2011. A protein complex network of Drosophila melanogaster. *Cell* **147**: 690–703.

Han KJ, Foster D, Harhaj EW, Dzieciatkowska M, Hansen K, Liu CW. 2016. Monoubiquitination of survival motor neuron regulates its cellular localization and Cajal body integrity. *Hum Mol Genet* **25**: 1392–1405.

Hosseinibarkooie S, Peters M, Torres-Benito L, Rastetter RH, Hupperich K, Hoffmann A, Mendoza-Ferreira N, Kaczmarek A, Janzen E, Milbradt J, et al. 2016. The Power of Human Protective Modifiers: PLS3 and CORO1C Unravel Impaired Endocytosis in Spinal Muscular Atrophy and Rescue SMA Phenotype. *Am J Hum Genet* **99**: 647–665.

Hsieh-Li HM, Chang JG, Jong YJ, Wu MH, Wang NM, Tsai CH, Li H. 2000. A mouse model for spinal muscular atrophy. *Nat Genet* **24**: 66–70.

Hsu SH, Lai MC, Er TK, Yang SN, Hung CH, Tsai HH, Lin YC, Chang JG, Lo YC, Jong YJ. 2010. Ubiquitin carboxyl-terminal hydrolase L1 (UCHL1) regulates the level of SMN expression through ubiquitination in primary spinal muscular atrophy fibroblasts. *Clin Chim Acta* **411**: 1920–1928.

Ikeda F, Dikic I. 2008. Atypical ubiquitin chains: new molecular signals. “Protein Modifications: Beyond the Usual Suspects” review series. *EMBO Rep* **9**: 536–542.

Jain AK, Barton MC. 2010. Making sense of ubiquitin ligases that regulate p53. *Cancer Biol Ther* **10**: 665–672.

Jiang J, Struhl G. 1998. Regulation of the Hedgehog and Wingless signalling pathways by the F-box/WD40-repeat protein Slimb. *Nature* **391**: 493–496.

Jin J, Ang XL, Shirogane T, Wade Harper J. 2005. Identification of substrates for F-box proteins. *Methods Enzymol* **399**: 287–309.

Kariya S, Park GH, Maeno-Hikichi Y, Leykekhman O, Lutz C, Arkovitz MS, Landmesser LT, Monani UR. 2008. Reduced SMN protein impairs maturation of the neuromuscular junctions in mouse models of spinal muscular atrophy. *Hum Mol Genet* **17**: 2552–2569.

Khush RS, Cornwell WD, Uram JN, Lemaitre B. 2002. A ubiquitin-proteasome pathway represses the Drosophila immune deficiency signaling cascade. *Curr Biol* **12**: 1728–1737.

Kim EK, Choi E. 2017. SMN1 functions as a novel inhibitor for TRAF6-mediated NF-κB signaling. *BBA - Mol Cell Res* **1864**: 760–770.

Kim TY, Siesser PF, Rossman KL, Goldfarb D, Mackinnon K, Yan F, Yi X, MacCoss MJ, Moon RT, Der CJ, et al. 2015. Substrate trapping proteomics reveals targets of the βTrCP2/FBXW11 ubiquitin ligase. *Mol Cell Biol* **35**: 167–181.

Kirkin V, McEwan DG, Novak I, Dikic I. 2009. A Role for Ubiquitin in Selective Autophagy. *Mol Cell* **34**: 259–269.

Kolb SJ, Kissel JT. 2015. Spinal Muscular Atrophy. *Neurol Clin* **33**: 831–846.

Komander D, Rape M. 2012. The Ubiquitin Code. *Annu Rev Biochem* **81**: 203–229.

Kong L, Wang X, Choe DW, Polley M, Burnett BG, Bosch-Marce M, Griffin JW, Rich MM, Sumner CJ. 2009. Impaired Synaptic Vesicle Release and Immaturity of Neuromuscular Junctions in Spinal Muscular Atrophy Mice. *J Neurosci* **29**: 842–851.

Korhonen L, Lindholm D. 2004. The ubiquitin proteasome system in synaptic and axonal degeneration: a new twist to an old cycle. *J Cell Biol* **165**: 27–30.

Kroiss M, Schultz J, Wiesner J, Chari A, Sickmann A, Fischer U. 2008. Evolution of an RNP assembly system: a minimal SMN complex facilitates formation of UsnRNPs in Drosophila melanogaster. *Proc Natl Acad Sci USA* **105**: 10045–10050.

Kwon DY, Dimitriadi M, Terzic B, Cable C, Hart AC, Chitnis A, Fischbeck KH, Burnett BG. 2013. The E3 ubiquitin ligase mind bomb 1 ubiquitinates and promotes the degradation of survival of motor neuron protein. *Mol Biol Cell* **24**: 1863–1871.

Kwon DY, Motley WW, Fischbeck KH, Burnett BG. 2011. Increasing expression and decreasing degradation of SMN ameliorate the spinal muscular atrophy phenotype in mice. *Hum Mol Genet* **20**: 3667–3677.

Le TT, Pham LT, Butchbach MER, Zhang HL, Monani UR, Coovert DD, Gavrilina TO, Xing L, Bassell GJ, Burghes AHM. 2005. SMNΔ7, the major product of the centromeric survival motor neuron (SMN2) gene, extends survival in mice with spinal muscular atrophy and associates with full-length SMN. *Hum Mol Genet* **14**: 845–857.

Lee YC, Liao PC, Liou YC, Hsiao M, Huang CY, Lu PJ. 2013. Glycogen synthase kinase 3 β activity is required for hBora/Aurora A-mediated mitotic entry. *Cell Cycle* **12**: 953–960.

Lefebvre S, Bürglen L, Reboullet S, Clermont O, Burlet P, Viollet L, Benichou B, Cruaud C, Millasseau P, Zeviani M, et al. 1995. Identification and characterization of a spinal muscular atrophy-determining gene. *Cell* **80**: 155–165.

Lefebvre S, Burlet P, Liu Q, Bertrandy S, Clermont O, Munnich A, Dreyfuss G, Melki J. 1997. Correlation between severity and SMN protein level in spinal muscular atrophy. *Nat Genet* **16**: 265–269.

Li DK, Tisdale S, Lotti F, Pellizzoni L. 2014. SMN control of RNP assembly: from post-transcriptional gene regulation to motor neuron disease. *Semin Cell Dev Biol*.

Li XM, Dong XP, Luo SW, Zhang B, Lee DH, Ting AKL, Neiswender H, Kim CH, Carpenter-Hyland E, Gao TM, et al. 2008. Retrograde regulation of motoneuron differentiation by muscle beta-catenin. *Nat Neurosci* **11**: 262–268.

Lim KL, Lim GGY. 2011. K63-linked ubiquitination and neurodegeneration. *Neurobiol Dis* **43**: 9–16.

Liu C, Li Y, Semenov M, Han C, Baeg GH, Tan Y, Zhang Z, Lin X, He X. 2002. Control of B-catenin phosphorylation/degradation by a dual-kinase mechanism. *Cell* **108**: 837–847.

Liu F, Walters KJ. 2010. Multitasking with ubiquitin through multivalent interactions. *Trends Biochem Sci* **35**: 352–360.

Liu M, Tu X, Ferrari-Amorotti G, Calabretta B, Baserga R. 2007. Downregulation of the upstream binding factor1 by glycogen synthase kinase3B in myeloid cells induced to differentiate. *J Cell Biochem* **100**: 1154–1169.

Lorson CL, Rindt H, Shababi M. 2010. Spinal muscular atrophy: mechanisms and therapeutic strategies. *Hum Mol Genet* **19**: R111–R118.

Lorson CL, Androphy EJ. 2000. An exonic enhancer is required for inclusion of an essential exon in the SMA-determining gene SMN. *Hum Mol Genet* **9**: 259–265.

Lorson CL, Hahnen E, Androphy EJ, Wirth B. 1999. A single nucleotide in the SMN gene regulates splicing and is responsible for spinal muscular atrophy. *Proc Natl Acad Sci USA* **96**: 6307–6311.

Makhortova NR, Hayhurst M, Cerqueira A, Sinor-Anderson AD, Zhao WN, Heiser PW, Arvanites AC, Davidow LS, Waldon ZO, Steen JA, et al. 2011. A screen for regulators of survival of motor neuron protein levels. *Nat Chem Biol* **7**: 544–552.

Marblestone JG, Butt S, McKelvey DM, Sterner DE, Mattern MR, Nicholson B, Eddins MJ. 2013. Comprehensive Ubiquitin E2 Profiling of Ten Ubiquitin E3 Ligases. *Cell Biochem Biophys* **67**: 161–167.

Martin R, Gupta K, Ninan NS, Perry K, Van Duyne GD. 2012. The Survival Motor Neuron Protein Forms Soluble Glycine Zipper Oligomers. *Structure* **20**: 1929–1939.

Matera AG, Wang Z. 2014. A day in the life of the spliceosome. *Nat Rev Mol Cell Biol* **15**: 108–121.

McWhorter ML, Monani UR, Burghes AHM, Beattie CE. 2003. Knockdown of the survival motor neuron (Smn) protein in zebrafish causes defects in motor axon outgrowth and pathfinding. *J Cell Biol* **162**: 919–931.

Meister G, Bühler D, Pillai R, Lottspeich F, Fischer U. 2001. A multiprotein complex mediates the ATP-dependent assembly of spliceosomal U snRNPs. *Nat Cell Biol* **3**: 1–8.

Monani UR, Sendtner M, Coovert DD, Parsons DW, Andreassi C, Le TT, Jablonka S, Schrank B, Rossoll W, Prior TW, et al. 2000. The human centromeric survival motor neuron gene (SMN2) rescues embryonic lethality in Smn(-/-) mice and results in a mouse with spinal muscular atrophy. *Hum Mol Genet* **9**: 333–339.

Monani UR. 2005. Spinal Muscular Atrophy: A Deficiency in a Ubiquitous Protein; a Motor Neuron-Specif Disease. *Neuron* **48**: 885–895.

Monani UR, Lorson CL, Parsons DW, Prior TW, Androphy EJ, Burghes AHM, McPherson JD. 1999. A single nucleotide difference that alters splicing patterns distinguishes the SMA gene SMN1 from the copy gene SMN2. *Hum Mol Genet* **8**: 1177–1183.

Mukhopadhyay D, Riezman H. 2007. Proteasome-independent functions of ubiquitin in endocytosis and signaling. *Science* **315**: 201–205.

Murase S, Mosser E, Schuman EM. 2002. Depolarization drives β-catenin into neuronal spines promoting changes in synaptic structure and function. *Neuron* **35**: 91–105.

Ning K, Drepper C, Valori CF, Ahsan M, Wyles M, Higginbottom A, Herrmann T, Shaw P, Azzouz M, Sendtner M. 2010. PTEN depletion rescues axonal growth defect and improves survival in SMN-deficient motor neurons. *Hum Mol Genet* **19**: 3159–3168.

Noureddine MA, Donaldson TD, Thacker SA, Duronio RJ. 2002. Drosophila Roc1a encodes a RING-H2 protein with a unique function in processing the Hh signal transducer Ci by the SCF E3 ubiquitin ligase. *Dev Cell* **2**: 757–770.

Ogino S, Wilson RB. 2004. Spinal muscular atrophy: molecular genetics and diagnostics. *Expert Rev Mol Diagn* **4**: 15–29.

O'Hearn PJ, Garcia EL, Le TH, Hart AC, Matera AG, Beattie CE. 2016. Non-mammalian animal models of SMA. In *Spinal Muscular Atrophy: Disease Mechanisms and Therapy* (eds. C. Sumner, S. Paushkin, and C.-P. Ko), pp. 221–239, Elsevier Academic Press, San Diego.

Ojeda L, Gao J, Hooten KG, Wang E, Thonhoff JR, Dunn TJ, Gao T, Wu P. 2011. Critical role of PI3k/Akt/GSK3β in motoneuron specification from human neural stem cells in response to FGF2 and EGF. *PLoS One* **6**.

Oprea GE, Kröber S, McWhorter ML, Rossoll W, Müller S, Krawczak M, Bassell GJ, Beattie CE, Wirth B. 2008. Plastin 3 is a protective modifier of autosomal recessive spinal muscular atrophy. *Science* **320**: 524–527.

Oskoui M, Darras B, De Vivo D. 2016. Spinal Muscular Atrophy: 125 Years Later and on the Verge of a Cure. In *Spinal Muscular Atrophy: Disease Mechanisms and Therapy* (eds. C. Sumner, S. Paushkin, and C.-P. Ko), pp. 3–17, Elsevier Academic Press, San Diego.

Paquette N, Broemer M, Aggarwal K, Chen L, Husson M, Ertürk-Hasdemir D, Reichhart JM, Meier P, Silverman N. 2010. Caspase-Mediated Cleavage, IAP Binding, and Ubiquitination: Linking Three Mechanisms Crucial for Drosophila NF-κB Signaling. *Mol Cell* **37**: 172–182.

Passini MA, Bu J, Roskelley EM, Richards AM, Sardi SP, O'Riordan CR, Klinger KW, Shihabuddin LS, Cheng SH. 2010. CNS-targeted gene therapy improves survival and motor function in a mouse model of spinal muscular atrophy. *J Clin Invest* **120**: 1253.

Patton EE, Willems AR, Sa D, Kuras L, Thomas D, Craig KL, Tyers M. 1998. Cdc53 is a scaffold protein for multiple Cdc34/Skp1/F-box protein complexes that regulate cell division and methionine biosynthesis in yeast. *Genes Dev* **12**: 692–705.

Patton EE, Willems A, Tyers M. 1998. Combinatorial control in ubiquitin-dependent proteolysis: don't Skp the F-box hypothesis. *Trends Genet* **14**: 236–243.

Pearn J. 1980. Classification of Spinal Muscular Atrophies. *Lancet* 919–922.

Pellizzoni L, Yong J, Dreyfuss G. 2002. Essential role for the SMN complex in the specificity of snRNP assembly. *Science* **298**: 1775–1779.

Petroski MD. 2008. The ubiquitin system, disease, and drug discovery. *BMC Biochem* **9**.

Pillai RS, Grimmler M, Meister G, Will CL, Lührmann R, Fischer U, Schümperli D. 2003. Unique Sm core structure of U7 snRNPs: Assembly by a specialized SMN complex and the role of a new component, Lsm11, in histone RNA processing. *Genes Dev* **17**: 2321–2333.

Praveen K, Wen Y, Gray KM, Noto JJ, Patlolla AR, Van Duyne GD, Matera AG. 2014. SMA-Causing Missense Mutations in Survival motor neuron (Smn) Display a Wide Range of Phenotypes When Modeled in Drosophila. *PLoS Genet* **10**: e1004489.

Praveen K, Wen Y, Matera AG. 2012. A Drosophila model of spinal muscular atrophy uncouples snRNP biogenesis functions of survival motor neuron from locomotion and viability defects. *Cell Rep* **1**: 624–631.

Prior TW. 2010. Spinal muscular atrophy: a time for screening. *Curr Opin Pediatr* **22**: 696–702.

Rajendra TK, Gonsalvez GB, Walker MP, Shpargel KB, Salz HK, Matera AG. 2007. A Drosophila melanogaster model of spinal muscular atrophy reveals a function for SMN in striated muscle. *J Cell Biol* **176**: 831–841.

Ramser J, Ahearn ME, Lenski C, Yariz KO, Hellebrand H, von Rhein M, Clark RD, Rindt H, Feng Z, Mazzasette C, Glascock JJ, Valdivia D, Pyles N, Crawford TO,

Rogers SL, Rogers GC. 2008. Culture of Drosophila S2 cells and their use for RNAi-mediated loss-of-function studies and immunofluorescence microscopy. *Nat Protoc* **3**: 606–611.

Rossoll W, Jablonka S, Andreassi C, Kroning AK, Karle K, Monani UR, Sendtner M. 2003. Smn, the spinal muscular atrophy-determining gene product, modulates axon growth and localization of beta-actin mRNA in growth cones of motoneurons. *J Cell Biol* **163**: 801–812.

Sanchez G, Dury AY, Murray LM, Biondi O, Tadesse H, El Fatimy R, Kothary R, Charbonnier F, Khandjian EW. 2013. A novel function for the survival motoneuron protein as a translational regulator. *Hum Mol Genet* **22**: 668–684.

Sareen D, O'Rourke JG, Meera P, Muhammad AKMG, Grant S, Simpkinson M, Bell S, Carmona S, Ornelas L, Sahabian A, et al. 2013. Targeting RNA foci in iPSC-derived motor neurons from ALS patients with a C9ORF72 repeat expansion. *Sci Transl Med* **5**: 1-13.

Schmutzler RK, Lichtner P, Hoffman EP, et al. 2008. Rare Missense and Synonymous Variants in UBE1 Are Associated with X-Linked Infantile Spinal Muscular Atrophy. *Am J Hum Genet* **82**: 188–193.

Schrank B, Gotz R, Gunnersen JM, Ure JM, Toyka KV, Smith AG, Sendtner M. 1997. Inactivation of the survival motor neuron gene, a candidate gene for human spinal muscular atrophy, leads to massive cell death in early mouse embryos. *Proc Natl Acad Sci* **94**: 9920–9925.

Shafey D, Côté PD, Kothary R. 2005. Hypomorphic Smn knockdown C2C12 myoblasts reveal intrinsic defects in myoblast fusion and myotube morphology. *Exp Cell Res* **311**: 49–61.

Sharma A, Lambrechts A, Hao LT, Le TT, Sewry CA, Ampe C, Burghes AHM, Morris GE. 2005. A role for complexes of survival of motor neurons (SMN) protein with

gemins and profilin in neurite-like cytoplasmic extensions of cultured nerve cells. *Exp Cell Res* **309**: 185–197.

Svendsen CN, Borg MG, Armstrong RJ, Rosser AE, Chandran S, Ostenfeld T, Caldwell MA. 1998. A new method for the rapid and long term growth of human neural precursor cells. *J Neurosci Methods* **85**: 141–152.

Swoboda KJ, Patitucci TN, Ebert AD, et al. 2015. Astrocytes influence the severity of spinal muscular atrophy. *Hum Mol Genet* **24**: 4094–4102.

Tan JMM, Wong ESP, Kirkpatrick DS, Pletnikova O, Ko HS, Tay SP, Ho MWL, Troncoso J, Gygi SP, Lee MK, et al. 2008. Lysine 63-linked ubiquitination promotes the formation and autophagic clearance of protein inclusions associated with neurodegenerative diseases. *Hum Mol Genet* **17**: 431–439.

Tiziano FD, Melki J, Simard LR. 2013. Solving the puzzle of spinal muscular atrophy: what are the missing pieces? *Am J Med Genet A* **161A**: 2836–2845.

Trinkle-Mulcahy L, Boulon S, Lam YW, Urcia R, Boisvert FM, Vandermoere F, Morrice NA, Swift S, Rothbauer U, Leonhardt H, et al. 2008. Identifying specific protein interaction partners using quantitative mass spectrometry and bead proteomes. *J Cell Biol* **183**: 223–239.

Valori CF, Ning K, Wyles M, Mead RJ, Grierson AJ, Shaw PJ, Azzouz M. 2010. Systemic delivery of scAAV9 expressing SMN prolongs survival in a model of spinal muscular atrophy. *Sci Transl Med* **2**: 35–42.

van Wijk SJL, Timmers HTM. 2010. The family of ubiquitin-conjugating enzymes (E2s): deciding between life and death of proteins. *FASEB J* **24**: 981–993.

Voigt T, Meyer K, Baum O, Schümperli D. 2010. Ultrastructural changes in diaphragm neuromuscular junctions in a severe mouse model for Spinal Muscular Atrophy and their prevention by bifunctional U7 snRNA correcting SMN2 splicing. *Neuromuscul Disord* **20**: 744–752.

Walker MP, Rajendra TK, Saieva L, Fuentes JL, Pellizzoni L, Matera AG. 2008. SMN complex localizes to the sarcomeric Z-disc and is a proteolytic target of calpain. *Hum Mol Genet* **17**: 3399–3410.

Wee CD, Kong L, Sumner CJ. 2010. The genetics of spinal muscular atrophies. *Curr Opin Neurol* **23**: 450–458.

Wirth B. 2000. An update of the mutation spectrum of the survival motor neuron gene (SMN1) in autosomal recessive spinal muscular atrophy (SMA). *Hum Mutat* **15**: 228–237.

Wishart TM, Mutsaers CA, Riessland M, Reimer MM, Hunter G, Hannam ML, Eaton SL, Fuller HR, Roche SL, Somers E, et al. 2014. Dysregulation of ubiquitin homeostasis and β-catenin signaling promote spinal muscular atrophy. *J Clin Invest* **124**: 1821–1834.

Ye Y, Rape M. 2009. Building ubiquitin chains: E2 enzymes at work. *Nat Rev Mol Cell Biol* **10**: 755–764.

Zhang L, Xu M, Scotti E, Chen ZJ, Tontonoz P. 2013. Both K63 and K48 ubiquitin linkages signal lysosomal degradation of the LDL receptor. *J Lipid Res* **54**: 1410–1420.

Zheng N, Schulman BA, Song L, Miller JJ, Jeffrey PD, Wang P, Chu C, Koepp DM, Elledge SJ, Pagano M, et al. 2002. Structure of the Cul1-Rbx1-Skp1-F boxSkp2 SCF ubiquitin ligase complex. *Nature* **416**: 703–709.

Zhou R, Silverman N, Hong M, Liao DS, Chung Y, Chen ZJ, Maniatis T. 2005. The role of ubiquitination in Drosophila innate immunity. *J Biol Chem* **280**: 34048–34055.

Gray_Fig1

A

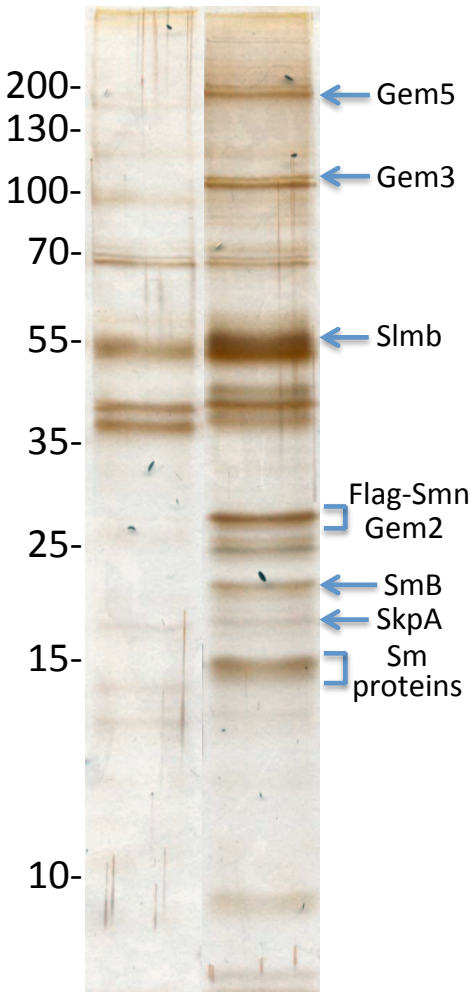

B

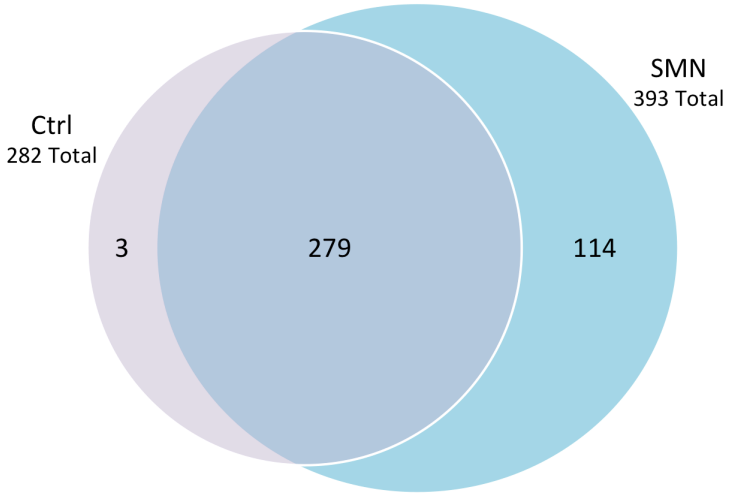

C

Protein	Gene #	Category	Intensity Ctrl (x10^5)	Intensity SMN (x10^5)	Peptides
Known SMN Interactors					
SMN	CG16725	SMN Complex	38.7	1415.2	9
Gem3	CG6539	SMN Complex	31.0	1052.2	31
Gem2	CG10419	SMN Complex	0.0	372.6	5
Gem5	CG30149	SMN Complex	0.0	96.5	16
SmE	CG18591	Sm protein	0.9	439.8	3
SmG	CG9742	Sm protein	0.4	364.5	6
SmD2	CG1249	Sm protein	0.0	303.4	5
SmF	CG16792	Sm protein	0.0	89.9	4
Lsm11	CG12924	Sm protein	0.0	47.3	8
SmD3	CG8427	Sm protein	0.3	31.1	2
SmD1	CG10753	Sm protein	0.0	20.0	3
SmB	CG5352	Sm protein	0.0	13.3	1
Lsm10	CG12938	Sm protein	0.0	11.2	2
Select Candidates					
Slmb	CG3412	UPS - SCF E3	0.7	253.6	13
SkpA	CG16983	UPS - SCF E3	3.4	91.1	5
Ben	CG18319	UPS - E2	2.1	27.3	5
Ubc2	CG6720	UPS - E2	2.9	9.2	2
Cul1	CG1877	UPS - SCF E3	0.0	8.0	4
UBE2S-like	CG8188	UPS - E2	0.0	5.8	3
Uch-L5	CG3431	UPS - DUB	1.1	4.5	2
Hyd	CG9484	UPS - E3	0.0	3.6	2
Cul5	CG1401	UPS - E3	0.0	2.8	2
Rpt1	CG1341	Proteasome	12.9	31.1	7
Rpt4	CG3455	Proteasome	8.8	29.2	6
Rpn2	CG11888	Proteasome	11.0	28.6	5
Rpn9	CG10230	Proteasome	6.5	23.0	5
Rpn6	CG10149	Proteasome	11.2	21.5	4
Rpn3	CG42641	Proteasome	2.7	15.3	5
Rpt3	CG16916	Proteasome	5.4	14.6	5
Rpn5	CG1100	Proteasome	6.0	13.2	4
Rpn11	CG18174	Proteasome	2.5	13.0	2
Rpn1	CG7762	Proteasome	1.9	11.0	5
Rpn7	CG5378	Proteasome	2.8	7.6	2
Rpn12	CG4157	Proteasome	2.5	5.2	3
CSN7	CG2038	COP9 signalosome	0.8	5.4	3
CSN3	CG18332	COP9 signalosome	0.0	3.7	2
CSN4	CG8725	COP9 signalosome	0.0	2.9	2
Sgg	CG2621	Kinase	2.2	9.8	4

D

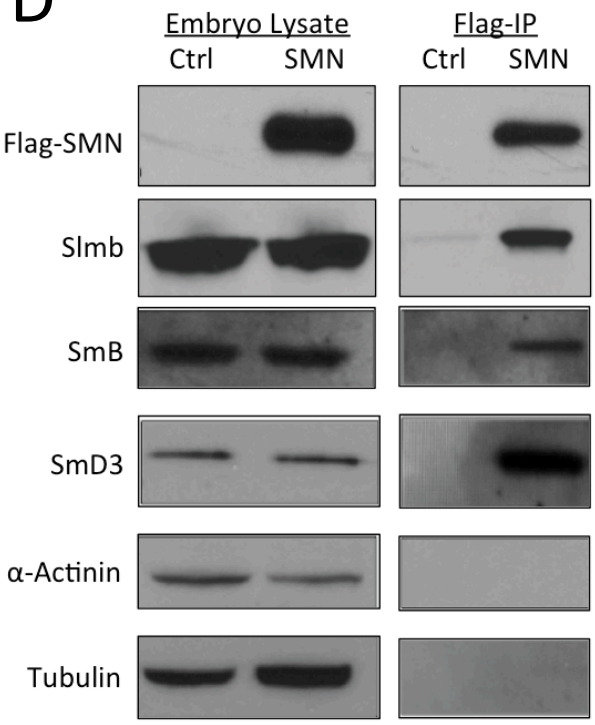

Gray_Fig2

A

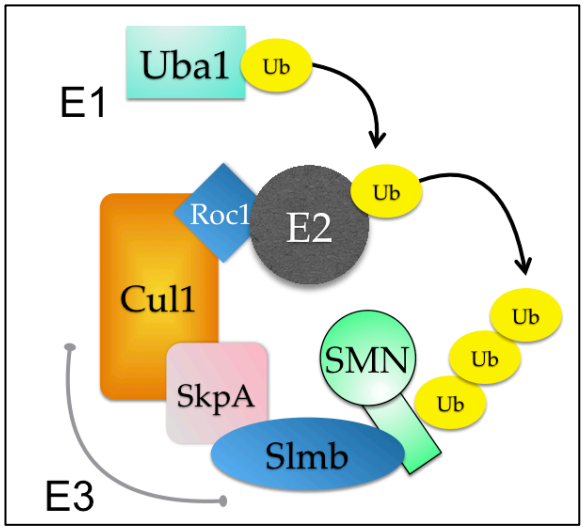

B

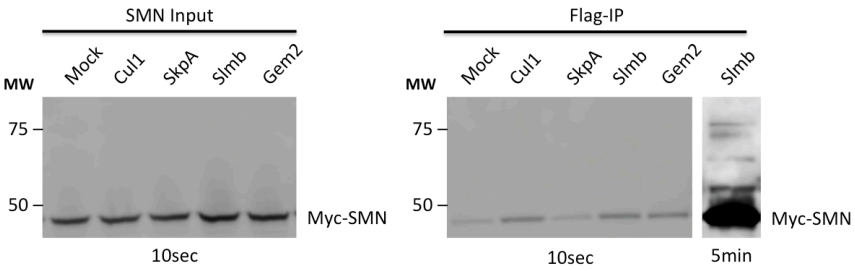

C

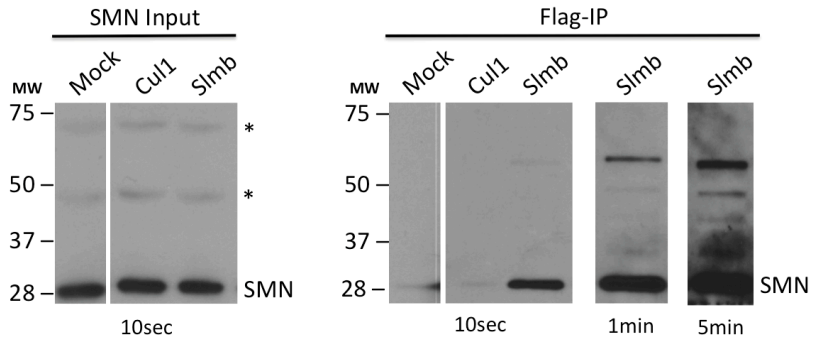

D

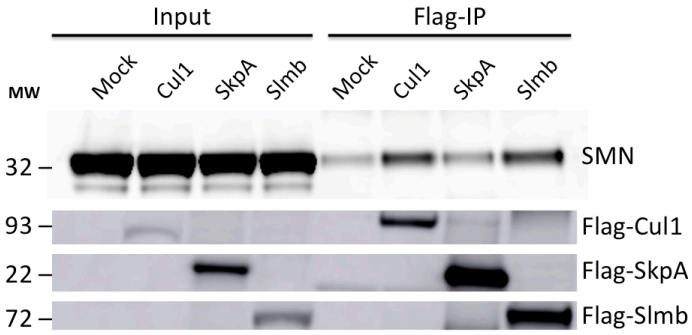

E

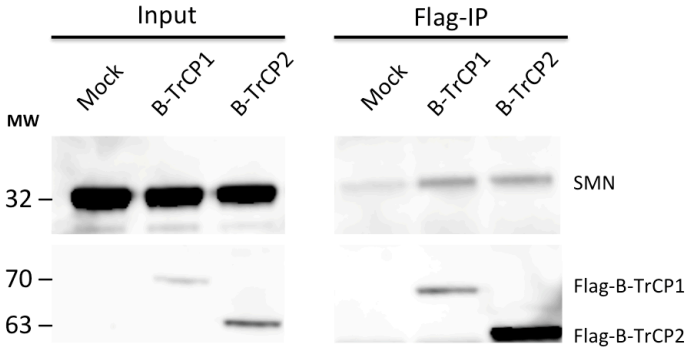

F

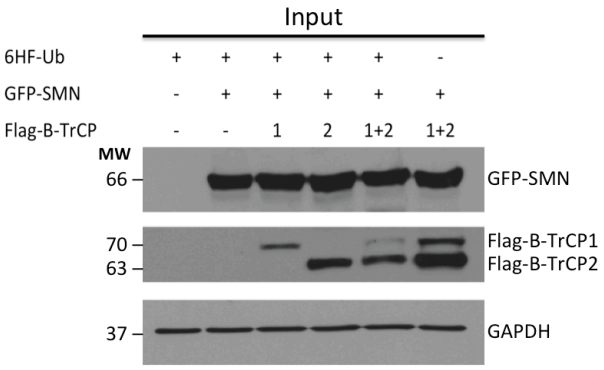

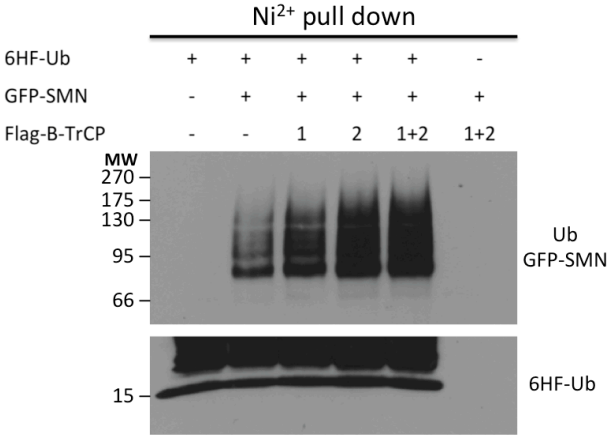

Gray_Fig3

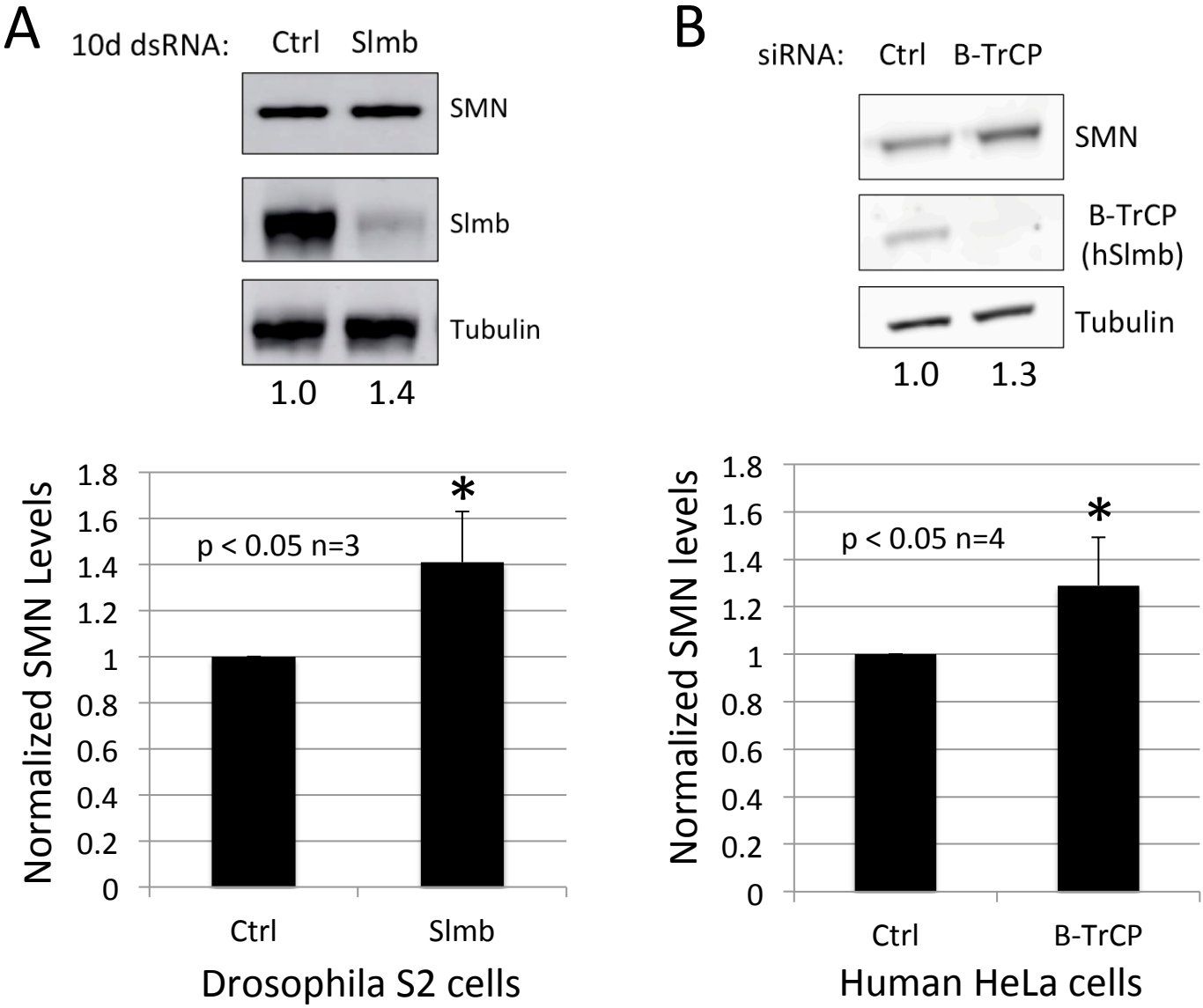
A
10d dsRNA:
Ctrl
Slmb
SMN
Slmb
Tubulin
1.0
1.4
Normalized SMN Levels
1.8
1.6
1.4
1.2
1
0.8
0.6
0.4
0.2
0
p < 0.05 n=3
*
Ctrl
Slmb
Drosophila S2 cells
B
siRNA:
Ctrl
B-TrCP
SMN
B-TrCP
(hSlmb)
Tubulin
1.0
1.3
Normalized SMN levels
1.8
1.6
1.4
1.2
1
0.8
0.6
0.4
0.2
0
p < 0.05 n=4
*
Ctrl
B-TrCP
Human HeLa cells

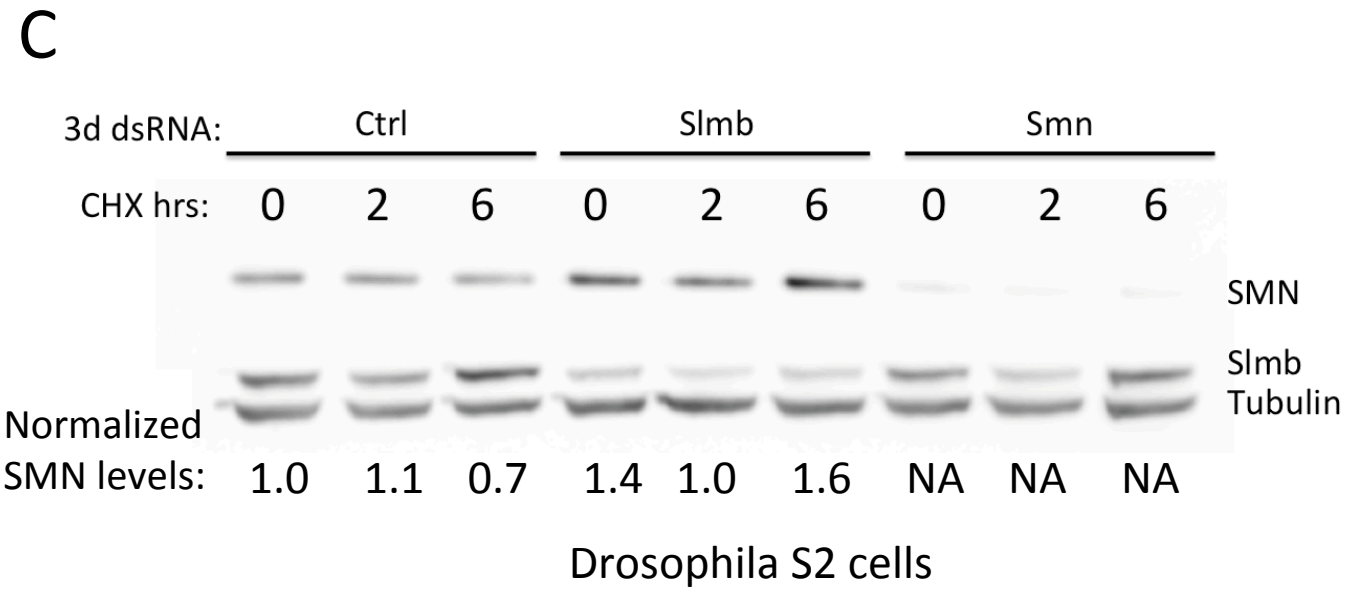
C
3d dsRNA:
Ctrl
Slmb
Smn
CHX hrs:
0
2
6
0
2
6
0
2
6
SMN
Slmb
Tubulin
Normalized
SMN levels:
1.0
1.1
0.7
1.4
1.0
1.6
NA
NA
NA
Drosophila S2 cells

Gray_Fig4

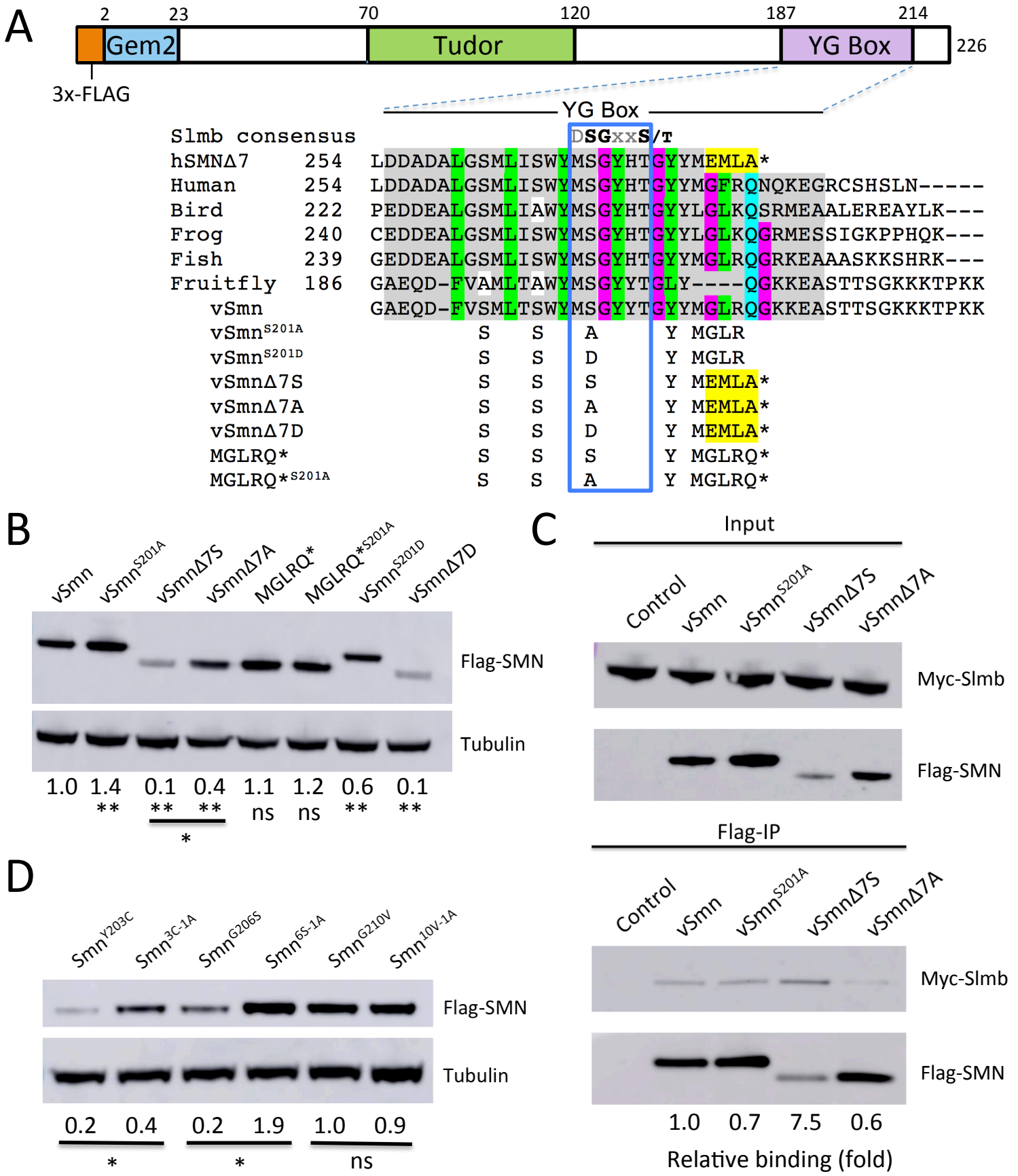
A
2
23
70
120
187
214
226
Gem2
Tudor
YG Box
3x-FLAG
YG Box
Slmb consensus DSGxxS/T
hSMNΔ7 254 LDDADALGSMLISWYMSGYHTGYYMEMLA*
Human 254 LDDADALGSMLISWYMSGYHTGYYMGFRQNQKEGRCSHSLN-----
Bird 222 PEDDEALGSMLIAWYMSGYHTGYYLGLKQSRMEAALEREAYLK---
Frog 240 CEDDEALGSMLISWYMSGYHTGYYLGLKQGRMESSIGKPPHQK---
Fish 239 GEDDEALGSMLISWYMSGYHTGYYMGLRQGRKEAAASKKSHRK---
Fruitfly 186 GAEQD-FVAMLTAWYMSGYYTGLY----QGKKEASTTSGKKKTPKK
vSmn GAEQD-FVSMLTSWYMSGYYTGYYMGLRQGKKEASTTSGKKKTPKK
vSmnS201A S S A Y MGLR
vSmnS201D S S D Y MGLR
vSmnΔ7S S S S Y MEMLA*
vSmnΔ7A S S A Y MEMLA*
vSmnΔ7D S S D Y MEMLA*
MGLRQ* S S S Y MGLRQ*
MGLRQ*S201A S S A Y MGLRQ*
B
vSmn
vSmnS201A
vSmnΔ7S
vSmnΔ7A
MGLRQ*
MGLRQ*S201A
vSmnS201D
vSmnΔ7D
Flag-SMN
Tubulin
1.0 1.4 0.1 0.4 1.1 1.2 0.6 0.1
** ** ** ns ns ** **
*
C
Input
Control
vSmn
vSmnS201A
vSmnΔ7S
vSmnΔ7A
Myc-Slmb
Flag-SMN
Flag-IP
Control
vSmn
vSmnS201A
vSmnΔ7S
vSmnΔ7A
Myc-Slmb
Flag-SMN
1.0 0.7 7.5 0.6
Relative binding (fold)
D
SmnY203C
Smn3C-1A
SmnG206S
Smn6S-1A
SmnG210V
Smn10V-1A
Flag-SMN
Tubulin
0.2 0.4 0.2 1.9 1.0 0.9
* * ns

Gray_Fig5

A

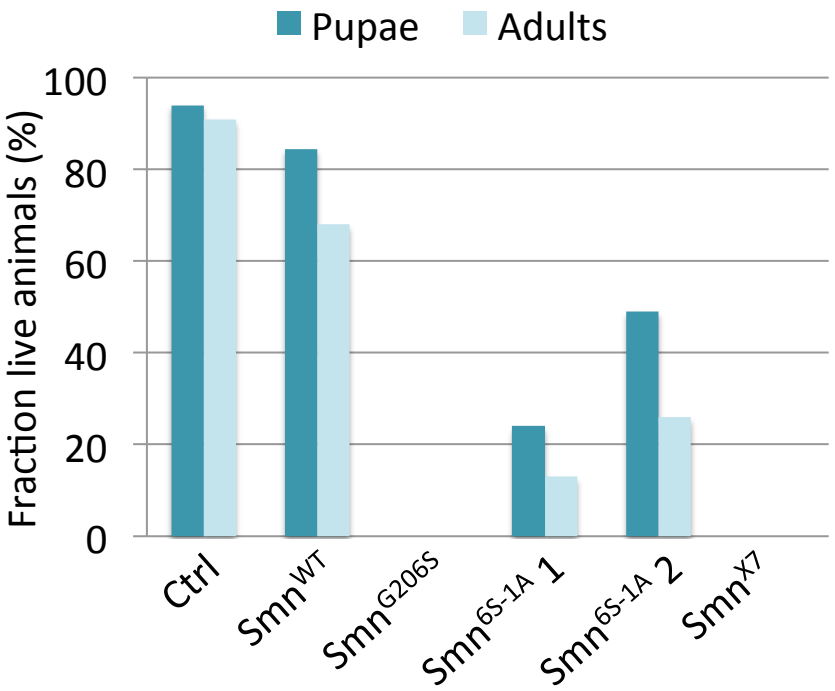

B

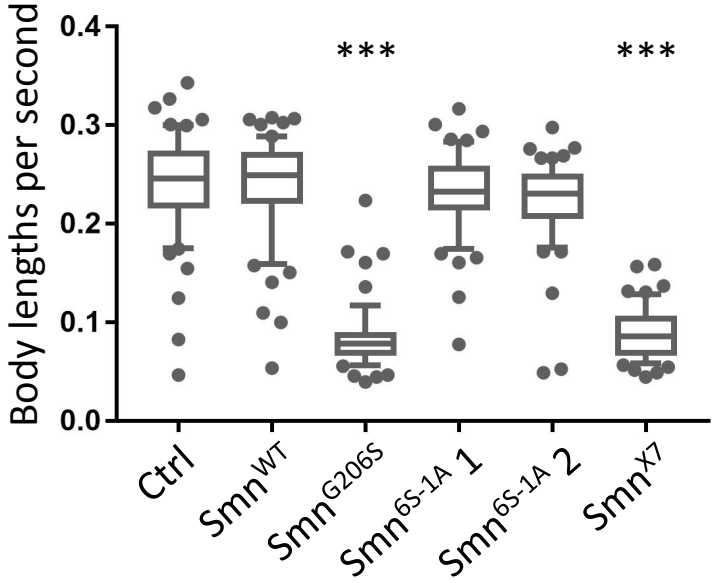

C

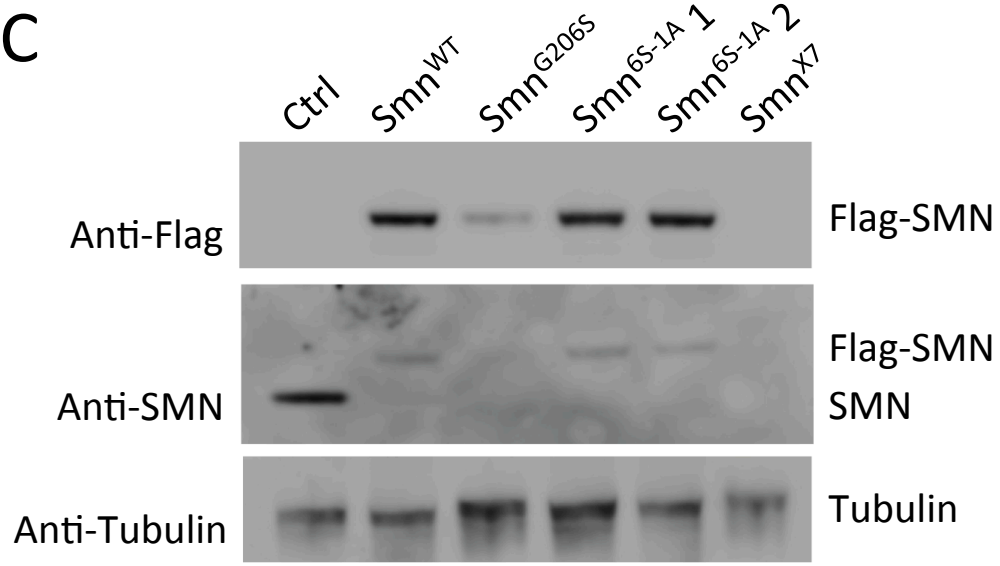

A

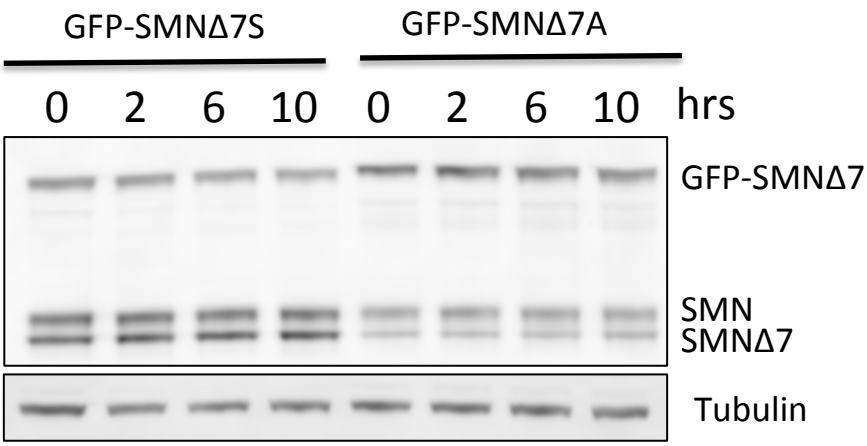

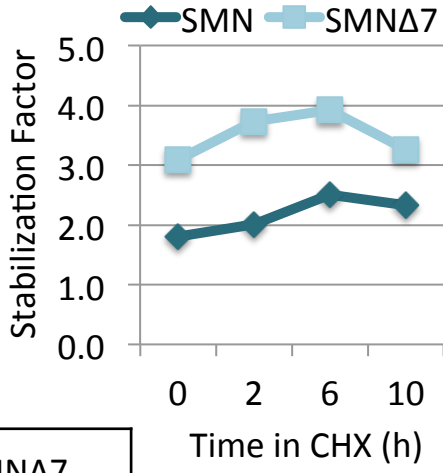

1.4	1.4	1.6	1.5	0.8	0.7	0.6	0.7	SMN/GFP-SMNΔ7
1.2	1.4	1.6	1.7	0.4	0.4	0.4	0.5	SMNΔ7/GFP-SMNΔ7

$$\textbf{Stabilization Factor} = \frac{\Delta 7S \text{ Intensity Ratio: (SMN or SMN}\Delta 7)/\text{GFP-SMN}\Delta 7S}{\Delta 7A \text{ Intensity Ratio: (SMN or SMN}\Delta 7)/\text{GFP-SMN}\Delta 7A} \quad \text{for each time point}$$

B

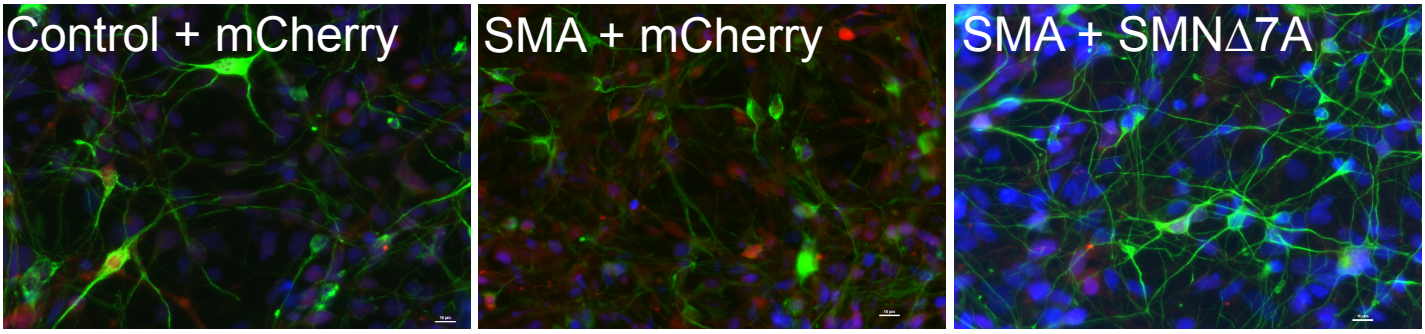

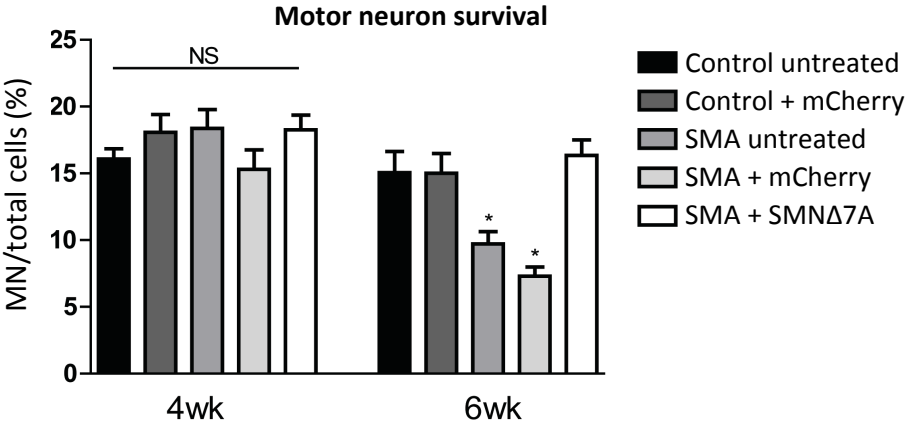

A

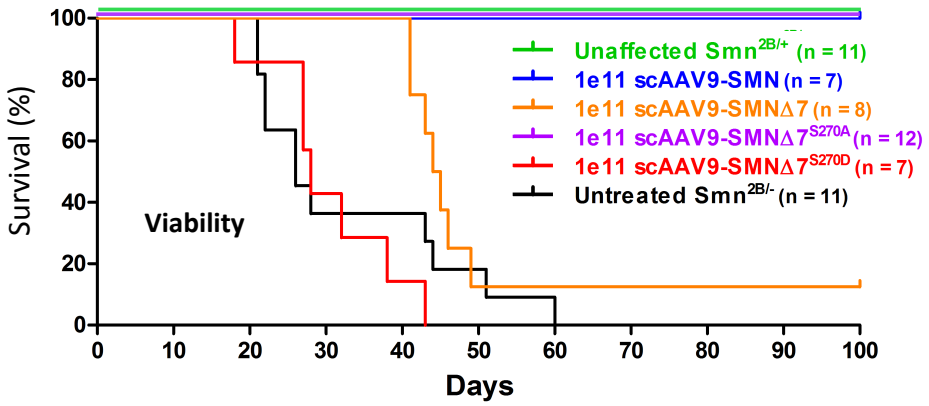
Survival (%)
Viability
Days
Unaffected Smn2B/+ (n = 11)
1e11 scAAV9-SMN (n = 7)
1e11 scAAV9-SMNΔ7 (n = 8)
1e11 scAAV9-SMNΔ7S270A (n = 12)
1e11 scAAV9-SMNΔ7S270D (n = 7)
Untreated Smn2B/- (n = 11)

B

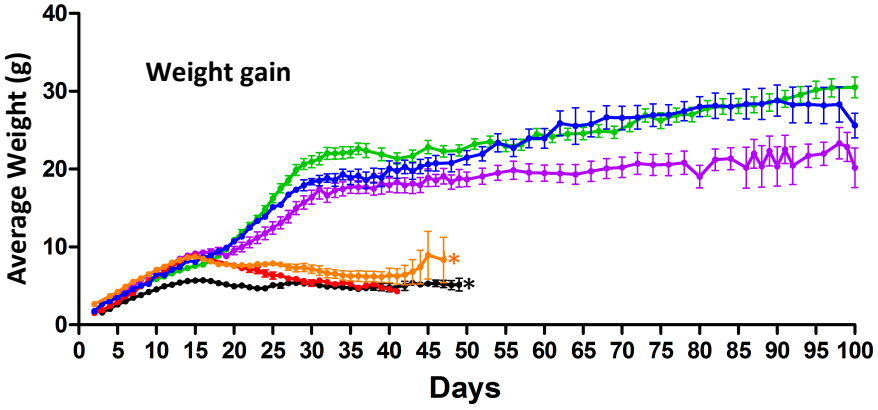
Average Weight (g)
Weight gain
Days

C

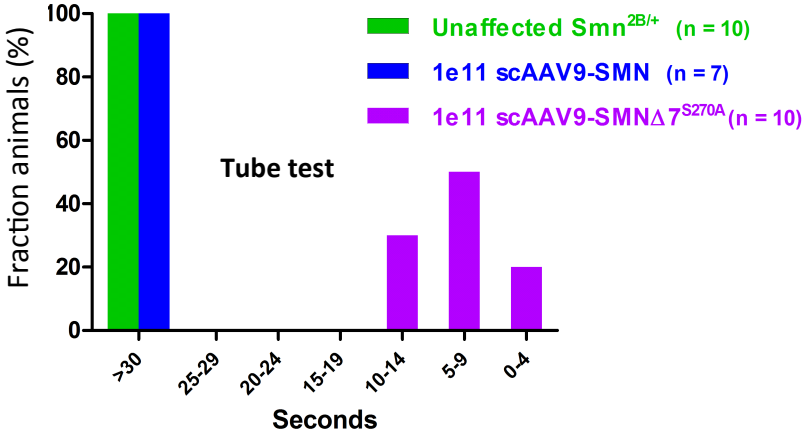
Fraction animals (%)
Tube test
Seconds
Unaffected Smn2B/+ (n = 10)
1e11 scAAV9-SMN (n = 7)
1e11 scAAV9-SMNΔ7S270A (n = 10)

S1

A

Genotype	Pupation (%)	Eclosion (%)
Smn^{WT}/Smn^{X7}	99	73
$vSmn/Smn^{X7}$	86	83
$vSmn^{S201A}/Smn^{X7}$	100	97.5

Figure S1: A) Transgenic flies expressing Flag-vSmn and Flag-$vSmn^{S201A}$ in the background of an *Smn^{X7}* null mutation are fully viable. The eclosion frequencies of these animals are consistently higher than those that express Flag-Smn^{WT} in the background of an *Smn^{X7}* null mutation. The data for each genotype are expressed as a fraction of pupae or adults over the total number of starting larvae, n=200.

S2

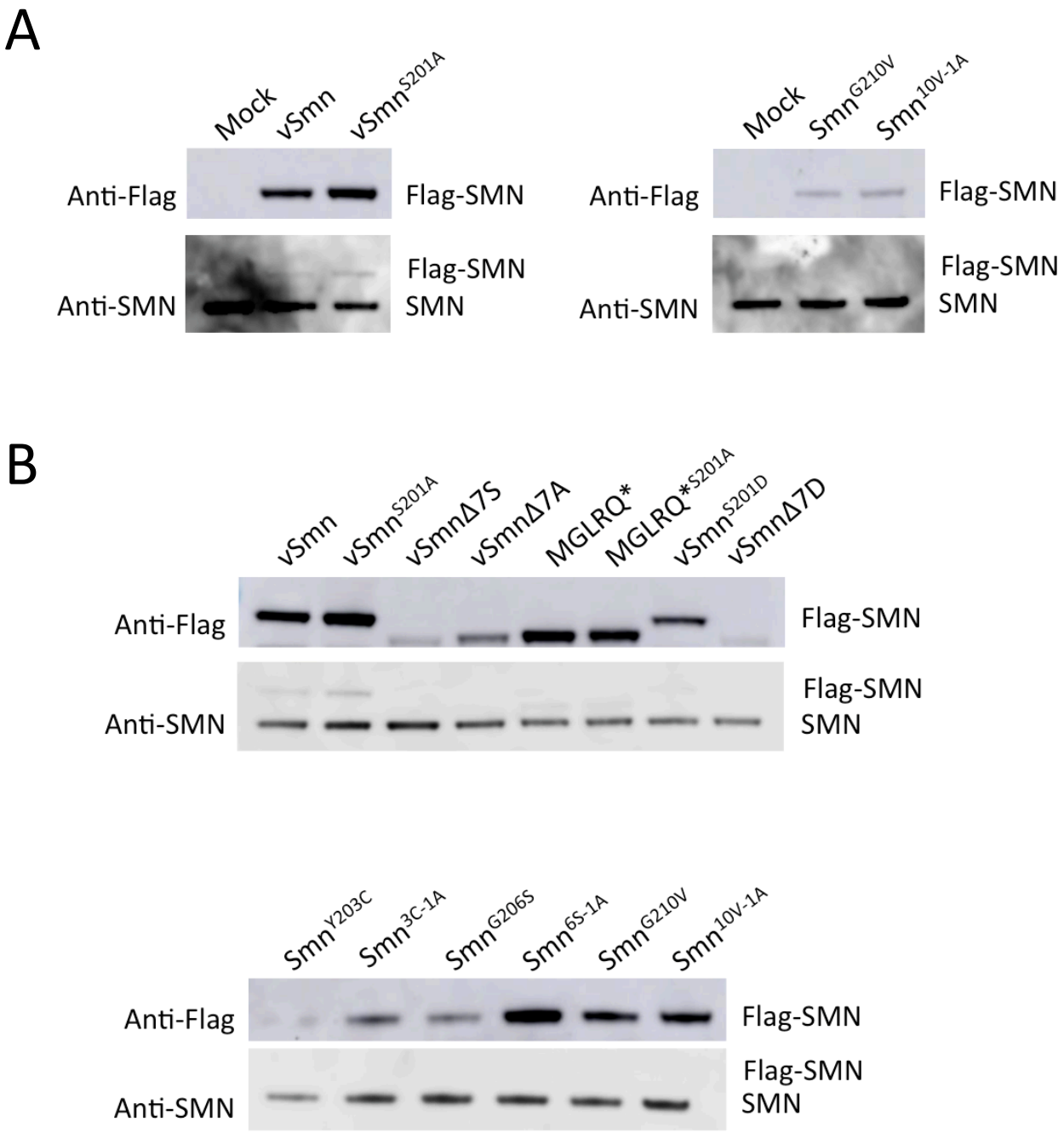

Figure S2: A) The expression of endogenous SMN in S2 cells following transient transfection of either modified SMN constructs (vSMN and vSMN^{S201A}) or Drosophila SMN constructs (G210V and G210V+S201A) is unaffected, as compared to mock transfection. B) Transient SMN transfections in S2 cells express Flag-SMN from the endogenous promoter. Protein levels of all transfected constructs are lower than endogenous SMN protein levels.

S3

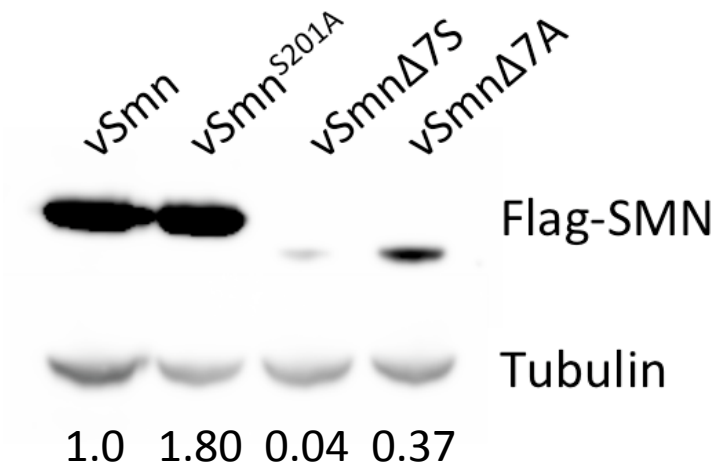

Figure S3: Protein lysates were made by pooling 40-50 adult flies. Levels of vSmnΔ7A in flies with one copy of the transgene and a balancer chromosome were relatively low. The vSmnΔ7S transgene was barely detectable in comparison to the full-length constructs (vSmn and vSmn^{S201A}). Flag-SMN was detected using anti-Flag antibody.

S4

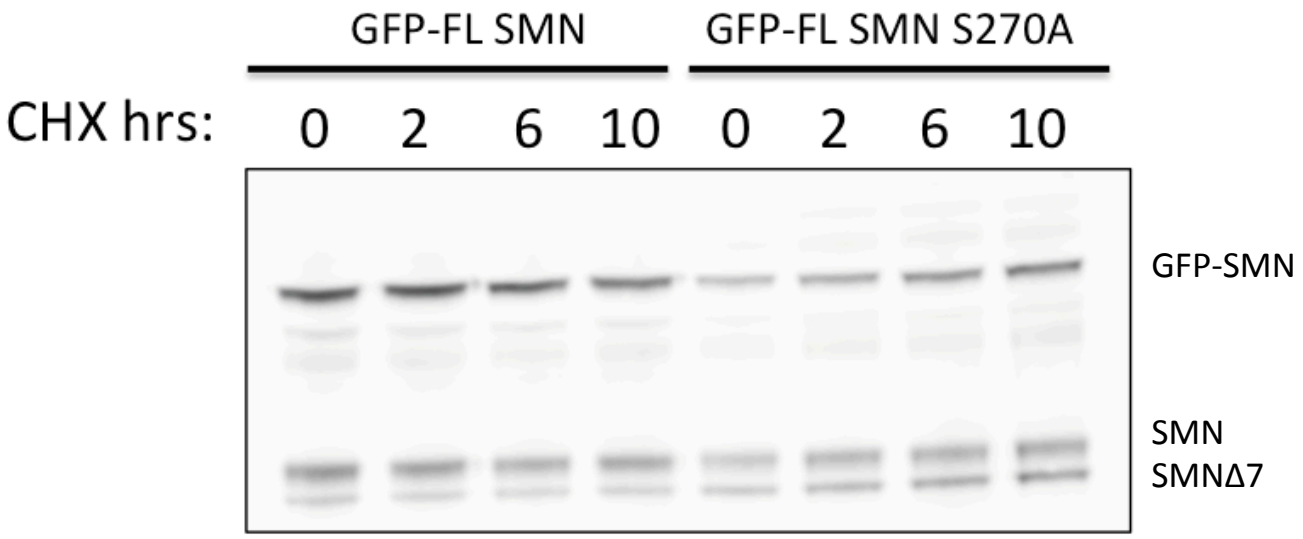

$$\textbf{Stabilization Factor (SF)} = \frac{\Delta 7S \text{ Intensity Ratio: (SMN or SMN}\Delta 7)/\text{GFP-SMN}}{\Delta 7A \text{ Intensity Ratio: (SMN or SMN}\Delta 7)/\text{GFP-SMN}^{S270A}}$$

$SF_{t=0}$: 0.22 for endogenous SMN and 0.63 for SMNΔ7

Figure S4: HEK 293T cells were transfected with equivalent amounts of GFP-SMN or –SMN^{S270A}. The following day, cells were harvested after treatment with cyclohexamide (CHX) for zero to ten hours. Western blotting with anti-SMN shows GFP-SMN, SMN and SMNΔ7. Stabilization factor was calculated as shown in Fig. 6A. For simplicity only calculation for time t=0 is shown.

S5

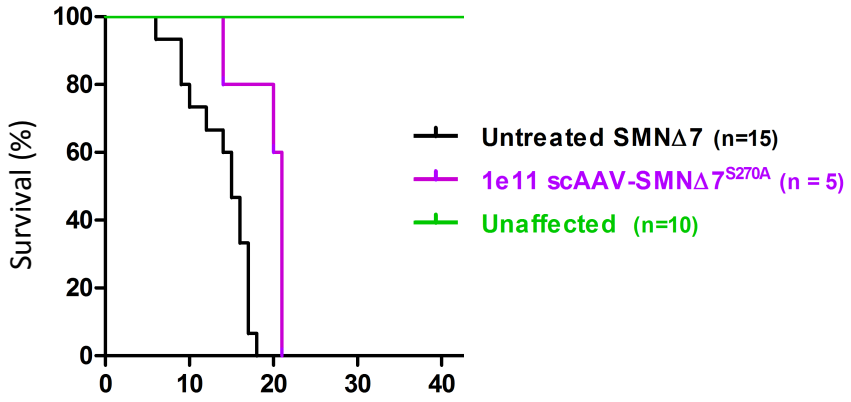

Figure S5: Survival analysis of the effects of SMNΔ7A expression in the severe Delta7 mouse model. Genotypes include untreated SMNΔ7 mice, which are a severe mouse model of SMA, SMNΔ7 mice treated with scAAV9 expressing SMNΔ7^{S270A}, truncated SMN with the S to A change in the degron, and control unaffected mice, which have a wild-type Smn allele. Treatment with AAV9-SMNΔ7A had only a very modest effect on viability and none of the animals survived weaning. 1e11 denotes the viral dose.

S6

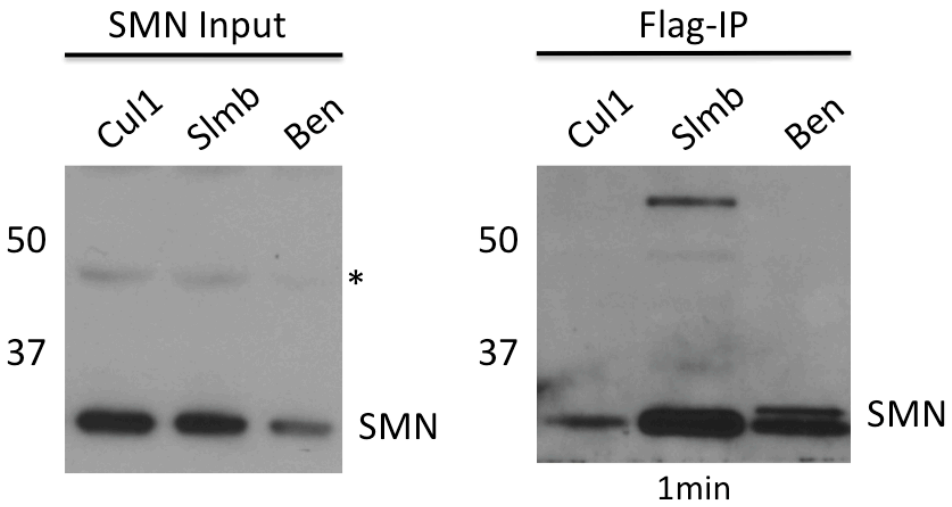

Figure S6: The interaction of SMN with Bendless (Ben) was validated in a co-immunoprecipitation assay. Flag-tagged Ben interacts with endogenous SMN in Drosophila S2 cells. SMN interaction with Flag-Slmb was used as a positive control for protein interaction. * is a non-specific band detected by the Drosophila SMN antibody.